

Synergising Hierarchical Data Centers and Power Networks: A Privacy-Preserving Approach

Junhong Liu, *Member, IEEE*, Fei Teng, *Senior Member, IEEE*, Yunhe Hou, *Senior Member, IEEE*

Abstract—In the era of digitization, data centers have emerged as integral contributors sustaining our interlinked world, bearing responsibility for an increasing proportion of the world's energy consumption. To facilitate the their fast rollout while progressing towards net-zero energy systems, the synergy of hierarchical data centers (cloud-fog-edge) and power networks can play a pivotal role. However, existing centralized co-dispatch manners encroach on the privacy of different agents within the integrated systems, meanwhile suffering from the combinatorial explosion. In this research, we propose a near-optimal distributed privacy-preserving approach to solve the non-convex synergy (day-ahead co-dispatch) problem. The synergy problem is formulated as a mixed integer quadratically constrained quadratic programming considering both communication and energy conservation, where Lyapunov optimization is introduced to balance operating costs and uncertain communication delays. To mitigate impacts of the highly non-convex nature, the normalized multi-parametric disaggregation technique is leveraged to reformulate the problem into a mixed integer non-linear programming. To further overcome non-smoothness of the reformulated problem, the customized ℓ_1 -surrogate Lagrangian relaxation method with convergence guarantees is proposed to solve the problem in a distributed privacy-preserving manner. The effectiveness, optimality, and scalability of the proposed methodologies for the synergy problem are validated via numerical simulations. Simulation results also indicate that computing tasks can be delayed and migrated within the hierarchical data centers, demonstrating the flexible resource allocation capabilities of the hierarchical data center architecture, further facilitating peak load balancing in the power network.

Index Terms—Bi-linear terms, Distributed non-convex optimization, Edge-fog-cloud computing, Lyapunov optimization, ℓ_1 -Surrogate Lagrangian decomposition

NOMENCLATURE

Abbreviations

<i>cal</i>	Calculation
<i>cha/dis</i>	Charge/discharge
<i>ess</i>	Energy storage system
<i>inf</i>	Infinity
<i>iot, fdc, cdc</i>	Internet of things (IoT), fog data center, cloud data center

<i>sup</i>	Supremum
<i>tran</i>	Transimission (for data flows)

Indices and Sets

τ	Index of time slot
e	Index of segments in RNMDT
i, i', j, m	Index of nodes/lines/agents

Junhong Liu and Yunhe Hou are with the Department of Electrical and Electronic Engineering, The University of Hong Kong, Hong Kong SAR, China (e-mail: jhliu, yhou@eee.hku.hk). (*Corresponding author: Yunhe Hou.*)

Fei Teng is with the Department of Electrical and Electronic Engineering, Imperial College London, London, UK (e-mail: f.teng@imperial.ac.uk).

k	Index of iterations
l, u	Index of lower/upper bounds for segments in RNMDT
$p(d)$	Index of nodes with power injections (data centers)
\mathcal{A}_j	Set of parent nodes for node j
\mathcal{C}_j	Set of child nodes for node j
\mathcal{D}	Set of total agents in the distributed optimization
\mathcal{N}	Set of total nodes
\mathcal{N}_g	Set of traditional thermal generators
\mathcal{N}_b	Set of branch lines
\mathcal{N}_{ess}	Set of energy storage systems
$\mathcal{N}_{iot/fdc/cdc}$	Set of IoT/fog/cloud data centers
\mathcal{N}_p	Set of nodes with power injections
\mathbb{Z}^-	Set of the negative integers
Parameters	
$\alpha_k/\theta/r/c$	Parameters for the Polyak step-size rule
β	Parameter for reaching an approximate linear rate
$\eta_{p(d)}^k$	Vector of penalty factors for the energy/communication coupling constraints at iteration k
η_p/η_d	Penalty factors for energy/communication coupling constraints, i.e., initially, 80, 200
η_{cha}/η_{dis}	Charging/Discharging efficient for the ess, i.e., 0.95, 0.95
κ_τ	Price of generating unit power for generators
$p_{j,\tau}^{dis}/p_{j,\tau}^{cha}$	Upper bound for discharging/charging of ess at the node j at time τ
π_τ	Price of charging/discharging unit power for generators/ess
$\sigma_{iot,tran}^2/\sigma_{fdc,tran}^2$	Noise power from IoT to fog data centers/from fog to cloud data centers, typically $-50 \sim -30$ dBm
τ_{cdc}	Maximum task latency in cloud data centers, i.e., 10s
$\Delta u_{j,\tau}$	Value of one segment for $H_{j,\tau}^{iot}$
$\Delta w_{j,\tau}$	Value of one segment for $H_{j,\tau}^{iot}$ multiplied by $U_{j,\tau}^{iot,cal}$
$\varpi_{i,d}, \varpi_{i',d}$	Mapping matrices of communication coupling constraints for the agent i/i'
$\varpi_{i,p}, \varpi_{i',p}$	Mapping matrices of energy coupling constraints for the agent i/i'
ϑ	Index of arbitrary segment in RNMDT
ξ^{iot}/ξ^{fdc}	Time slot length for the IoT/fog data centers, i.e., 1, 1 ms
ξ^k	Stepsize for distributed update at iteration k
ζ_j	Power usage effectiveness (PUE), i.e., 1.4

d^{iot}/d^{fdc}	Calculation density of IoT/fog data centers, where processing one bit of the data needs d CPU cycle frequencies, typically $5000cycle/bit$	\mathcal{T}	penalty terms, i.e., 1.01
$f_{j,\tau}^{iot/fdc,min}/f_{j,\tau}^{iot/fdc,max}$	Lower/Upper bound of CPU operating frequency of IoT/fog data center j at time τ , i.e., $0, 0.5 \times 10^9, 5 \times 10^9 cycle/s$	$\mathcal{W}_{j,\tau}^{iot,tran}/\mathcal{W}_{j,\tau}^{fdc,tran}$	Total number of time slots Channel bandwidth from IoT to fog data centers/from fog to cloud data centers, typically 40MHz
$g_{j,\tau}^{iot,tran}/g_{j,\tau}^{fdc,tran}$	Transmitting power from IoT to fog data centers/from fog to cloud data centers, typically uniform distribution $U(0, 1) \times 2 W$	Variables	
$h_{j,\tau}^{iot,tran}/h_{j,\tau}^{fdc,tran}$	Channel gain from IoT to fog data centers/from fog to cloud data centers, typically $-5 \sim -2$	$\mathbf{x}_{i,\tau}$	Vector of decision variables for each agent i at time τ
$H_{j,\tau}^u/H_{j,\tau}^l$	Upper/Lower bound of $H_{j,\tau}^{iot}$	γ_p^k/γ_d^k	Primal/Dual residual at iteration k
$H_{j,max}^{iot/fog}$	Maximum volumes of data queues for IoT/fog data centers, i.e., 10, 10 Mb/ms	$\Delta u_{j,\tau}/\Delta w_{j,\tau}$	Convex hull for the segment of one variable/the segmented multiplication of two variables for IoT data center j at time τ
I_j	Bit amount per task request per time slot arriving at the cloud server j , i.e., 2.5 request/Mb	$\Delta(H_{j,\tau}^{iot})$	Lyapunov drift term for data queue from IoT data center j at time τ
k^{iot}/k^{fdc}	Capacitance switching coefficient determined by the chip architecture of IoT/fog data centers, typically $1.7 \times 10^{-27}, 1.6 \times 10^{-27} W * s^3/cycle^3$	$\hat{C}_j^{iot}/\hat{C}_j^{fdc}$	Total approximate cost for the IoT/fog data center j at time τ
k_1, k_2	Lower/Upper bound of segments for the integer variable in RNMDT	B_{iot}/B_{fdc}	Constant part of the Lyapunov drift for the queue at IoT/fog data center
$l_{ij,\tau}^{min}/l_{ij,\tau}^{max}$	Lower/Upper bound of power current on the line ij at time τ	$f_{j,\tau}^{iot}/f_{j,\tau}^{fdc}$	CPU operating frequency of IoT/fog data centers j at time τ
$M_{j,cdc}$	Number of servers in cloud data center j , i.e., 500	$H_{j,\tau}^{iot}/H_{j,\tau}^{fdc}$	Queue of tasks at the IoT/fog data center j at time τ
$P_{ij,\tau}^{min}/P_{ij,\tau}^{max}$	Lower/Upper bound of active power flow on the line ij at time τ	$n_{j,\tau}/\mu_{j,\tau}/\lambda_{j,\tau}$	Number of working servers/Utilization rate/Total income bit amount of tasks at the cloud data center j at time τ
$p_{j,\tau}^r$	Active power for the renewable generator at the node j at time τ	$P_{ij,\tau}/Q_{ij,\tau}/l_{ij,\tau}$	Active power/Reactive power/Current flow over the line ij at time τ
$p_{j,\tau}^{min}/p_{j,\tau}^{max}$	Lower/Upper bound of nodal active power injection of node j at time τ	$p_{j,\tau}/q_{j,\tau}$	Active/Reactive power injection of node j at time τ
P_{peak}/P_{idle}	Peak/Idle power consumption of cloud data centers' IT equipment, i.e., 500, 200W	$p_{j,\tau}^g/p_{j,\tau}^{dis}/p_{j,\tau}^{cha}$	Active power for the generator/discharging of ess/charging of ess at the node j at time τ
$Q_{ij,\tau}^{min}/Q_{ij,\tau}^{max}$	Lower/Upper bound of reactive power flow on the line ij at time τ	$p_{j,\tau}^{fdc,cal}/p_{j,\tau}^{fdc,tran}$	Power consumed for local task computation/transmission of fog data center j at time τ
$q_{j,\tau}^{min}/q_{j,\tau}^{max}$	Lower/Upper bound of nodal reactive power injection of node j at time τ	$p_{j,\tau}^{iot,cal}/p_{j,\tau}^{iot,tran}$	Power consumed for local task computation/transmission of IoT data center j at time τ
$r_{ij}/x_{ij}/z_{ij}$	Resistance/Reactance/Impedance of the line ij	$p_{j,\tau}^{iot/fdc/cdc}$	Active power for the IoT/fog/cloud data centers at the node j at time τ
$R_{j,\tau}^{down}/R_{j,\tau}^{up}$	Limits for ramping down/up for generator j at time τ	$p_{j,\tau}^{iot}/p_{j,\tau}^{fdc}$	Total Power consumed for task processing of IoT/fog data center j at time τ
$R_{j,\tau}^{iot,tran}/R_{j,\tau}^{fdc,tran}$	Data transmission rate from IoT to fog data centers/from fog to cloud data centers	$S_{j,\tau}^{ess}$	State of charge for ess j at time τ
$S_{j,\tau}^{min}/S_{j,\tau}^{max}$	Lower/Upper bound of state of the charge for the ess j at time τ , i.e., 0, 10 MWh	$U_{j,\tau}^{fdc,cal}/U_{j,\tau}^{fdc,tran}$	Bit amount of tasks calculated at/transmitted from fog data center j at time τ
$S_{j,\tau}^{iot}$	Incoming task requests at IoT data center j at time τ	$U_{j,\tau}^{iot,cal}/U_{j,\tau}^{iot,tran}$	Bit amount of tasks calculated at/transmitted from IoT data center j at time τ
V_{iot}/V_{fdc}	Hyper-parameters helping balance the economic benefit and stability of queues, i.e., 0.0008, 0.005	$v_{j,\tau}$	Squared voltage magnitude of node j at time τ
$v_{j,\tau}^{min}/v_{j,\tau}^{max}$	Lower/Upper bound of squared voltage magnitude of node j at time τ	z_e^{cdc}/\hat{n}_e	Discrete variable for each segment e /Value of the segmented multiplication of two variables for cloud data center j at time τ
w	Parameter for adaptively adjusting the	$z_{j,\tau}^{cha}$	Charging state of ess j at time τ
		$z_{j,e,\tau}^{iot}/\hat{y}_{j,e,\tau}$	Discrete variable for each segment e /Value of the segmented multiplication of two variables for IoT data center j at time τ

$\mathcal{C}_j^{iot}/\mathcal{C}_j^{f^{dc}}$ Total original cost for the IoT/fog data center j at time τ

Functions

$\mathcal{P}/\mathcal{P}_\emptyset$ Original optimization function/Extended real-value function

$L(H_{j,\tau}^{iot})$ Lyapunov function for data queue from IoT data center j at time τ

$\mathcal{J}(\cdot)/\mathcal{J}_{i,\tau}(\cdot)$ Objective function/Agent-based objective function for agent i at time τ of the reformulated problem by Lyapunov optimization

$\mathcal{L}_\eta(\cdot)/\mathcal{L}_{\eta,i}(\cdot)$ Augmented Lagrangian function/Augmented Lagrangian function for agent i with penalty term η

I. INTRODUCTION

DATA centers serve as the foundational infrastructure supporting a myriad of activities across economic and technological domains. Fueled by data-intensive innovations such as artificial intelligence and 5G devices, data centers operate at a high capacity to meet diverse computing requests. Cloud computing is a centralized model where data is stored and processed at a remote data center, while the confluence of data proliferation and long physical distance between cloud data centers and devices can lead to the violation of bandwidth constraints and latency issues [1]. To address these challenges, the adoption of Internet of things (IoT) edge and fog data centers has emerged as a prominent solution [2]. For instance, Google Inc. launched the Distributed Cloud in 2021, extending its cloud infrastructure to the edge and customer data centers [3]. Edge data centers are strategically positioned closely to end-users, enabling the delivery of rapid edge computing services with minimal latency. Edge computing aims to minimize the volume of data transferred to the cloud data center, thereby reducing the network latency. Moreover, fog data centers co-located with routers in the local network further extend the capabilities of edge computing by providing an intermediary layer of computing infrastructure between edge devices and the cloud data center. Nevertheless, heterogeneity of the hierarchical computing paradigm, i.e., edge-fog-cloud computing, raises multiple challenges, e.g., where to offload the workloads (from the edge or fog servers) and how to meet the quality of service (QoS) requirements [4]. Meanwhile, substantial surge in the digital contents is transforming data centers into one of the fastest-growing consumers of electricity, whose global demand is 299 TWh in 2020 and is estimated to reach 848 TWh in 2030 [5]. Therefore, enhancing energy efficiency of data centers is paramount to reach the carbon neutrality by 2060, requiring coordinated dispatch of the hierarchical data centers and power networks [6].

The prevailing approach for data centers to collaboratively evolve with power networks involves their participation in demand response programs. Researchers have proposed data center-grid coupling models considering queuing theory and job scheduling techniques [7], the data-driven assessment scheme of data centers [8], prediction-based pricing with analytic and worst-case bounds [9], robust bi-level co-optimization model [10], four-level joint optimal dispatch

model [6] to promote the active participation of data centers in demand response programs. The potential benefits of data centers engaging in demand response services are analyzed in [11], with results demonstrating up to a 40% reduction in data center operational costs. The aforementioned optimization problems for power networks with data centers are primarily addressed in a centralized manner. However, optimization models for the co-dispatch problem must acknowledge the unavailability of information within data centers to power systems and also the issue of curse of dimension introduced by integer variables [12], [13]. Meanwhile, the overall energy efficiency of hierarchical edge-fog-cloud data centers have rarely been investigated. Addressing these challenges necessitates a systematic solution that respects the interests and privacy of data centers while ensuring overall computational efficiency.

Currently, numerous distributed algorithms have been proposed to solve optimization problems in the integrated energy systems while preserving data privacy, such as the optimal condition decomposition (OCD) [14], alternating direction method of multipliers (ADMM) [15], auxiliary problem principle (APP) [16], augmented lagrangian alternating direction inexact newton (ALADIN) [17]. Among them, ADMM-based approaches have garnered widespread attention for the optimization problems of integrated energy systems due to their strong convergence performance. For instance, ADMM is employed for the the online distributed energy management of data centers [18], [19]. Reference [13] proposed a learning-aided ADMM algorithm for the decentralized optimization for integrated electricity-heat systems with data centers. Nevertheless, these works consider the simplified convex data center models and only focus on the real-time operation of data centers. Moreover, to enhance privacy preservation across data centers, differential privacy techniques have been proposed to obscure sensitive information [20], [21]. However, these approaches are typically applied at the individual data center level, overlooking the coordination and synergy required at the system-wide scale.

To facilitate the synergy (co-dispatch) of hierarchical data centers and power networks, the optimization problem can be inherently modeled as the mixed integer non-linear programming (MINLP). However, the classic distributed algorithms, i.e., OCD, ADMM, APP, ALADIN, can not handle the non-convex MINLP due to the co-existence of mixed integers and non-linearity [22]. While ALADIN has been reported to perform effectively for the nonlinear programming (NLP), it remains challenging to guarantee the convergence of mixed integer programming (MIP) [23]. Beyond the aforementioned distributed algorithms, researchers proposed customized distributed algorithms for solving the optimization problem with integer variables. The ℓ_1 -augmented Lagrangian method (ALM) with additional shares of non-convex reverse norm cuts is proposed for the two-block mixed integer linear programming (MILP) [24]. Nevertheless, the effectiveness of this method diminishes as the problems scale increases, since it requires the preservation of all historical cuts as constraints. Additionally, SDM-GS-ALM is proposed for solving MILP in a distributed manner [25], [26]. Moreover, to enhance the performance of SDM-GS-ALM, reference [27], [28] further

proposed the VILS algorithm, which adaptively selects inner loop iterations in the computation of Lagrangian upper bounds, rather than relying on pre-fixed inner loop iterations as in SDM-GS-ALM. However, both SDM-GS-ALM and VILS algorithms require a linear cost function and the construction of a convex hull for integer variables to ensure convergence.

Nevertheless, several characteristics define the synergy problem of hierarchical data centers and power networks, representing a more general and realistic case in the dispatch/operation of integrated power networks: 1) a potentially large number of integer variables, resulting in the high combinatorial complexity; 2) a non-linear objective function; 3) the presence of discrete variables within the sub-problems. These properties pose obstacles for the applicability of existing distributed algorithms and research. Specifically, the potentially large number of integer variables necessitates sharing numerous non-convex reverse norm cuts for the ℓ_1 -ALM, which diminishes the effectiveness of this method. Meanwhile, the non-linear objective function renders both the SDM-GS-ALM and VILS theoretically inapplicable. Furthermore, the presence of potentially large number of discrete variables within the sub-problems poses significant challenges for employing the ADMM. To overcome these challenges, we propose a set of methodologies inspired by [29] to solve the large-scale MIQCQP in a privacy-preserving manner. Specifically, to address the non-convex and non-smooth nature of the synergy problem, we propose reformulating the original synergy problem into a MINLP by leveraging the novel reformulated normalized multiparametric disaggregation technique (RNMDT). This reformulation enhances computational efficiency in solving the synergy problem while guaranteeing near-optimality from both theoretical and experimental perspectives. To overcome non-smoothness of the reformulated problem, the customized ℓ_1 -surrogate Lagrangian relaxation method with convergence guarantees is proposed to solve the problem in a distributed privacy-preserving manner. Surrogate subgradient directions are constructed via the surrogate optimality conditions to form acute angles with directions toward the optimal multipliers. With adaptively adjusted stepsizes, multipliers tend to optimal ones, facilitating the attainment of optimal solutions of the non-smooth MINLP problem. The main contributions are summarized as follows:

- We formulate the day-ahead co-dispatch problem of hierarchical data center penetrated power networks as a mixed integer quadratically constrained quadratic programming (MIQCQP) considering both communication and energy conservation, where Lyapunov optimization is introduced to minimize operating costs while stabilizing uncertain data queues in the communication network.
- The highly non-convex synergy problem is reformulated into a mixed integer non-linear programming (MINLP) by leveraging the reformulated normalized multi-parametric disaggregation technique, which can be made arbitrarily precise via a precision parameter.
- To further overcome combinatorial explosion and preserve privacy for agents, we propose the customized ℓ_1 -surrogate Lagrangian relaxation method with convergence guarantees to solve the non-smooth MINLP in

a distributed privacy-preserving manner, which employs surrogate optimality conditions and adaptively adjusted stepsizes to generate search directions that form acute angles toward the optimal multipliers.

The remainder of this paper is organized as follows: Section II introduces the centralized co-dispatch problem of hierarchical data centers integrated power networks and its nearly exact reformulations. Section III proposes a distributed privacy-preserving approach for solving the co-dispatch problem. Section IV demonstrates the effectiveness of the proposed approach with case studies. Section V draws the conclusions.

II. FORMULATIONS OF THE EDGE-FOG-CLOUDS PENETRATED POWER SYSTEMS

A. Centralized Co-Dispatch Problem of Hierarchical Data Centers Penetrated Power Networks

As illustrated in Fig. 1, this paper considers the day-ahead co-dispatch problem for the hierarchical data centers and distribution power networks [30], [31], which operate at low to medium voltage levels. In this framework, hierarchical data centers and storage systems are modeled as flexible loads, while distributed generators supply electricity within the distribution system. The day-ahead market prices, determined at the transmission level, are employed to facilitate the buying/selling of additional electricity between the distribution network and bulk power grid. The synergy problem is formulated as:

$$\begin{aligned} \min_{\mathbf{x}} \quad & \sum_{\tau \in \mathcal{T}} \left\{ \sum_{j \in \mathcal{N}_g} \kappa_{\tau} p_{j,\tau}^g + \sum_{j \in \mathcal{N}_{ess}} \pi_{\tau} (p_{j,\tau}^{cha} - p_{j,\tau}^{dis}) + \right. \\ & \left. \sum_{j \in \mathcal{N}_{cdc}} \pi_{\tau} p_{j,\tau}^{cdc} + \sum_{ij \in \mathcal{N}_b} r_{ij} l_{ij,\tau} \right\} + \sum_{j \in \mathcal{N}_{iot}} c_j^{iot} + \sum_{j \in \mathcal{N}_{fdc}} c_j^{fdc} \end{aligned} \quad (1a)$$

$$\text{s.t.} \quad \sum_{m \in \mathcal{C}_j} P_{jm,\tau} - \sum_{i \in \mathcal{A}_j} (P_{ij,\tau} - r_{ij} l_{ij,\tau}) = p_{j,\tau}, j \in \mathcal{N}_p \quad (1b)$$

$$\sum_{m \in \mathcal{C}_j} Q_{jm,\tau} - \sum_{i \in \mathcal{A}_j} (Q_{ij,\tau} - x_{ij} l_{ij,\tau}) = q_{j,\tau}, j \in \mathcal{N}_p \quad (1c)$$

$$v_{j,\tau} = v_{i,\tau} - 2(r_{ij} P_{ij,\tau} + x_{ij} Q_{ij,\tau}) + z_{ij} l_{ij,\tau}, j \in \mathcal{N}_p \quad (1d)$$

$$P_{ij,\tau}^2 + Q_{ij,\tau}^2 \leq l_{ij,\tau} v_{i,\tau}, ij \in \mathcal{N}_b \quad (1e)$$

$$p_{j,\tau}^{\min} \leq p_{j,\tau} \leq p_{j,\tau}^{\max}, j \in \mathcal{N}_p \quad (1f)$$

$$q_{j,\tau}^{\min} \leq q_{j,\tau} \leq q_{j,\tau}^{\max}, j \in \mathcal{N}_p \quad (1g)$$

$$v_{j,\tau}^{\min} \leq v_{j,\tau} \leq v_{j,\tau}^{\max}, j \in \mathcal{N}_p \quad (1h)$$

$$l_{ij,\tau}^{\min} \leq l_{ij,\tau} \leq l_{ij,\tau}^{\max}, ij \in \mathcal{N}_b \quad (1i)$$

$$0 \leq p_{j,\tau}^{cha} \leq z_{j,\tau}^{cha} \overline{p_{j,\tau}^{cha}}, j \in \mathcal{N}_{ess} \quad (1j)$$

$$0 \leq p_{j,\tau}^{dis} \leq (1 - z_{j,\tau}^{cha}) \overline{p_{j,\tau}^{dis}}, j \in \mathcal{N}_{ess} \quad (1k)$$

$$S_{j,\tau+1}^{ess} = S_{j,\tau}^{ess} + p_{j,\tau}^{cha} \eta_{cha} - p_{j,\tau}^{dis} / \eta_{dis}, j \in \mathcal{N}_{ess} \quad (1l)$$

$$S_{j,\tau}^{min} \leq S_{j,\tau}^{ess} \leq S_{j,\tau}^{max}, j \in \mathcal{N}_{ess} \quad (1m)$$

$$p_{j,\tau}^{g,min} \leq p_{j,\tau}^g \leq p_{j,\tau}^{g,max}, j \in \mathcal{N}_g \quad (1n)$$

$$p_{j,\tau+1}^g - p_{j,\tau}^g \leq R_{j,\tau}^{up}, j \in \mathcal{N}_g \quad (1o)$$

$$p_{j,\tau-1}^g - p_{j,\tau}^g \leq R_{j,\tau}^{down}, j \in \mathcal{N}_g \quad (1p)$$

$$p_{j,\tau}^g + p_{j,\tau}^r + p_{j,\tau}^{dis} - p_{j,\tau}^{cha} - p_{j,\tau}^{iot,fdc,cdc} = p_{j,\tau}, j \in \mathcal{N}, \quad (1q)$$

where $z_{j,\tau}^{cha}$ is the binary variable. κ_{τ} is the per unit generation cost, and π_{τ} is the predicted locational marginal price. The

objective function (1a) is to minimize the total operation cost or, equivalently, maximize the social welfare, which contains six parts: i) the first item models the generation cost; ii) the second item models the expense of charging/discharging electricity by the energy storage system; iii) the third term models the cost of purchasing electricity by the IoT edge data center; iv) the fourth term models the cost of purchasing electricity by the fog data center; v) the fifth term models the cost of purchasing electricity by the cloud data center; vi) the sixth term models the power loss within the system [32]. The non-convex constraint in Distflow model is relaxed through the second order cone programming (SOCP) as in (1e), which is an exact reformulation for radial networks when power loss minimization is considered [33], [34]. As denoted in (1q), active power injections at each bus are modeled to ensure energy conservation depending on the existence of the generator, renewable generator, energy storage system, IoT edge data center, fog data center, and cloud data center.

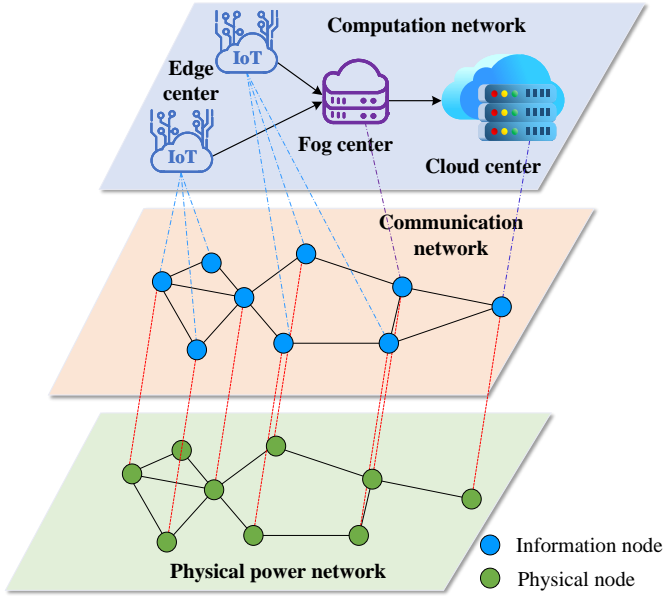


Fig. 1. Synergy of the hierarchical data centers and power networks.

According to [2], the three-tier hierarchical data centers, i.e., IoT edge–fog–cloud data centers, can be constructed as in Fig. 2. Power consumed at the IoT edge data center, i.e., $p_{j,\tau}^{fdc}$, consists of two parts: i) the power consumed for local computation at edge data center, i.e., $p_{j,\tau}^{iot,cal}$; ii) power consumed for task transmission from IoT to fog data centers, i.e., $p_{j,\tau}^{iot,tran}$. Meanwhile, power consumed at the fog data center also consists of two parts: i) power consumed for local computation at the fog data center, i.e., $p_{j,\tau}^{fdc,cal}$; ii) and power consumed for task transmission from fog to cloud data centers, i.e., $p_{j,\tau}^{fdc,tran}$. The power consumption for IoT edge and fog data centers can be modelled as:

$$p_{j,\tau}^{iot,cal} = k^{iot} U_{j,\tau}^{iot,cal} d^{iot} (f_{j,\tau}^{iot})^2 \quad (2a)$$

$$f_{j,\tau}^{iot,min} \leq f_{j,\tau}^{iot} \leq f_{j,\tau}^{iot,max} \quad (2b)$$

$$0 \leq U_{j,\tau}^{iot,cal} \leq \frac{f_{j,\tau}^{iot,max} \xi^{iot}}{d^{iot}} \quad (2c)$$

$$p_{j,\tau}^{iot,tran} = \frac{U_{j,\tau}^{iot,tran} g_{j,\tau}^{iot,tran}}{R_{j,\tau}^{iot,tran}} \quad (2d)$$

$$R_{j,\tau}^{iot,tran} = W_{j,\tau}^{iot,tran} \log_2 \left(1 + \frac{h_{j,\tau}^{iot,tran} g_{j,\tau}^{iot,tran}}{\sigma_{iot,tran}^2} \right) \quad (2e)$$

$$0 \leq U_{j,\tau}^{iot,tran} \leq R_{j,\tau}^{iot,tran} \xi^{iot} \quad (2f)$$

$$H_{j,\tau+1}^{iot} = H_{j,\tau}^{iot} - U_{j,\tau}^{iot,cal} - U_{j,\tau}^{iot,tran} + S_{j,\tau}^{iot} \quad (2g)$$

$$0 \leq U_{j,\tau}^{iot,cal} + U_{j,\tau}^{iot,tran} \leq H_{j,\tau}^{iot} \quad (2h)$$

$$\lim_{\tau \rightarrow +\infty} \frac{\mathbb{E}(H_{j,\tau}^{iot})}{T} = 0 \quad (2i)$$

$$p_{j,\tau}^{fdc,cal} = k^{fdc} U_{j,\tau}^{fdc,cal} d^{fdc} (f_{j,\tau}^{fdc})^2 \quad (2j)$$

$$f_{j,\tau}^{fdc,min} \leq f_{j,\tau}^{fdc} \leq f_{j,\tau}^{fdc,max} \quad (2k)$$

$$0 \leq U_{j,\tau}^{fdc,cal} \leq \frac{f_{j,\tau}^{fdc,max} \xi^{fdc}}{d^{fdc}} \quad (2l)$$

$$p_{j,\tau}^{fdc,tran} = \frac{U_{j,\tau}^{fdc,tran} g_{j,\tau}^{fdc,tran}}{R_{j,\tau}^{fdc,tran}} \quad (2m)$$

$$R_{j,\tau}^{fdc,tran} = W_{j,\tau}^{fdc,tran} \log_2 \left(1 + \frac{h_{j,\tau}^{fdc,tran} g_{j,\tau}^{fdc,tran}}{\sigma_{fdc,tran}^2} \right) \quad (2n)$$

$$0 \leq U_{j,\tau}^{fdc,tran} \leq R_{j,\tau}^{fdc,tran} \xi^{fdc} \quad (2o)$$

$$H_{j,\tau+1}^{fdc} = H_{j,\tau}^{fdc} - U_{j,\tau}^{fdc,cal} - U_{j,\tau}^{fdc,tran} + U_{j,\tau}^{iot,tran} \quad (2p)$$

$$0 \leq U_{j,\tau}^{fdc,cal} + U_{j,\tau}^{fdc,tran} \leq H_{j,\tau}^{fdc} \quad (2q)$$

$$\lim_{\tau \rightarrow +\infty} \frac{\mathbb{E}(H_{j,\tau}^{fdc})}{T} = 0 \quad (2r)$$

$$p_{j,\tau}^{iot} = p_{j,\tau}^{iot,cal} + p_{j,\tau}^{iot,tran} \quad (2s)$$

$$C_j^{iot} = \lim_{\tau \rightarrow +\infty} \frac{1}{T} \sum_{\tau \in T} \mathbb{E}(\pi_{\tau} p_{j,\tau}^{iot}) \quad (2t)$$

$$p_{j,\tau}^{fdc} = p_{j,\tau}^{fdc,cal} + p_{j,\tau}^{fdc,tran} \quad (2u)$$

$$C_j^{fdc} = \lim_{\tau \rightarrow +\infty} \frac{1}{T} \sum_{\tau \in T} \mathbb{E}(\pi_{\tau} p_{j,\tau}^{fdc}) \quad (2v)$$

$$H_{j,max}^{iot} \geq H_{j,\tau}^{iot} \geq 0, H_{j,max}^{fdc} \geq H_{j,\tau}^{fdc} \geq 0, \quad (2w)$$

where (2f) and (2o) model the amount of data that can be transferred via the communication channel between IoT edge and fog data centers, and the communication channel between fog and cloud data centers, respectively. Constraints (2d) and (2m) model the power consumption of transferring data for IoT edge and fog data centers, which depend on the data transmission rates, i.e., $R_{j,\tau}^{iot,tran}$ and $R_{j,\tau}^{fdc,tran}$ [35]. For the data transmission, the wireless communication is considered due to the emergence of 5G/6G technologies in the distribution power network [36]. However, the energy consumption associated with the wireless transmission is non-negligible. The Shannon-Hartley formula captures the relation between energy consumption in wireless uplink channels and the data transmission rate, as denoted by formulas (2e) and (2n). This formula has been widely adopted in existing research [37], [38]. Formulas (2a) and (2j) model the energy consumption for processing tasks at the IoT and fog data centers, respectively. Compared to the energy consumed for processing tasks at local data centers, the power required for transmitting data to remote data centers is much lower. However, both types

of energy consumption are non-negligible. Formulas (2g) and (2p) model the data queues from the IoT to fog data centers and that from the fog to cloud data centers, respectively. $H_{j,\tau}^{iot}$ and $H_{j,\tau}^{fdc}$ are the data buffer queues exist in the two communication channels, which follows first-in-first-out rule. Due to the potentially uncertain communication demands within each dispatch time-slot, i.e., one hour, the expected costs for IoT edge and fog data centers are employed as in (2t) and (2v). To avoid large deviation from the expected state, the real-time optimization method should be considered within each dispatch time-slot to correct the scheduling plan [39].

For the cloud data center, approximately 40% of energy consumption comes from cooling systems and the remaining consumption is from the information technology (IT) facilities. Normally the energy consumption of IT facilities is modeled and an additional coefficient, i.e., power usage effectiveness (PUE) denoted by ζ_j , is multiplied to derive the overall energy consumption [40]. More detailed energy consumption models for cloud data centers are also possible [41], including the IT computer rack power, power delivery loss from the power distribution units (PDUs) to the racks, the power for lights, and the power consumed to operate the cooling system. However, incorporating such models introduces additional non-linearity into the synergy problem, posing significant challenges for solving the overall optimization problem. Meanwhile, the average time delay of task requests at cloud data center follows the M/M/1 queue theory [42]. The modeling of cloud data center follows as:

$$\lambda_{j,\tau}/I_j \leq n_{j,\tau} \leq M_{j,cdc}, n_{j,\tau} \in \mathbb{Z}^+ \quad (3a)$$

$$0 \leq \mu_{j,\tau} \leq 1 \quad (3b)$$

$$\lambda_{j,\tau} = \sum_{i \in \mathcal{N}_{fdc}} U_{i,\tau}^{fdc,tran} \quad (3c)$$

$$0 \leq \frac{1}{\mu_{j,\tau} - \frac{\lambda_{j,\tau}}{n_{j,\tau} I_j}} \leq \tau_{cdc} \quad (3d)$$

$$p_{j,\tau}^{cdc} = [(P_{peak} - P_{idle})\mu_{j,\tau}n_{j,\tau} + M_{j,cdc}P_{idle}] \cdot \zeta_j, \quad (3e)$$

where $n_{j,\tau}$ is the number of servers in working conditions and $\mu_{j,\tau}$ is the server utilization rate. $\lambda_{j,\tau}$ is the total incoming computing request at time slot τ of cloud data center j .

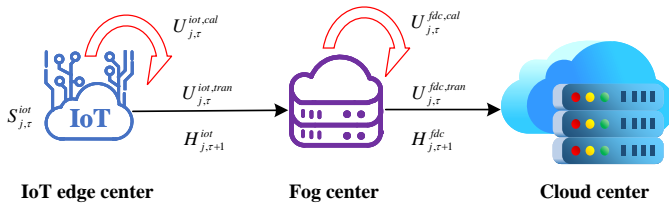


Fig. 2. Task allocation of the hierarchical edge-fog-cloud computing.

B. Lyapunov Optimization based Corrective Strategy

For the online corrective strategy, Lyapunov optimization method exhibits superior performance and lower computational complexity compared to other online methods, e.g., online convex optimization and model predictive control [43]. Therefore, the real-time online optimization method, i.e.,

Lyapunov optimization method, is introduced to reformulate the synergy problem with a three-tier data center structure. Accordingly, limit operations in the objective function as well as constraints (2i) and (2r) can be avoided following the method, enabling the problem to be directly handled by commercial solvers. The Lyapunov function and the Lyapunov drift [44] are employed to define the stability of data queues as:

$$L(H_{j,\tau}^{iot}) := \frac{1}{2}(H_{j,\tau}^{iot})^2 \quad (4a)$$

$$\Delta(H_{j,\tau}^{iot}) := L(H_{j,\tau+1}^{iot}) - L(H_{j,\tau}^{iot}). \quad (4b)$$

Lemma 1: The Lyapunov drift term for data queue from IoT edge data center, i.e., $\Delta_{H_{j,\tau}^{iot}}$, can be upper bounded as follow:

$$\Delta(H_{j,\tau}^{iot}) \leq B_{iot} + H_{j,\tau}^{iot}[S_{j,\tau}^{iot} - U_{j,\tau}^{iot,cal} - U_{j,\tau}^{iot,tran}], \quad (5)$$

where B_{iot} is a constant value.

Proof: The following relation can be derived according to the definition of Lyapunov drift:

$$\begin{aligned} \Delta(H_{j,\tau}^{iot}) &= \frac{1}{2}(H_{j,\tau+1}^{iot})^2 - \frac{1}{2}(H_{j,\tau}^{iot})^2 \\ &= \frac{1}{2}(S_{j,\tau}^{iot} - U_{j,\tau}^{iot,cal} - U_{j,\tau}^{iot,tran})^2 \\ &\quad + H_{j,\tau}^{iot}[S_{j,\tau}^{iot} - U_{j,\tau}^{iot,cal} - U_{j,\tau}^{iot,tran}] \\ &\leq B_{iot} + H_{j,\tau}^{iot}[S_{j,\tau}^{iot} - U_{j,\tau}^{iot,cal} - U_{j,\tau}^{iot,tran}], \end{aligned} \quad (6)$$

where B_{iot} represents the upper bound for the term $\frac{1}{2}(S_{j,\tau}^{iot} - U_{j,\tau}^{iot,cal} - U_{j,\tau}^{iot,tran})^2$. Similarly, we can obtain the upper bound of the Lyapunov drift for the data queue from the fog data center to cloud data center as:

$$\begin{aligned} \Delta(H_{j,\tau}^{fdc}) &\leq B_{fdc} \\ &\quad + H_{j,\tau}^{fdc}[U_{j,\tau}^{iot,tran} - U_{j,\tau}^{fdc,cal} - U_{j,\tau}^{fdc,tran}]. \end{aligned} \quad (7)$$

Based on the obtained upper bounds, the objective function for IoT edge and fog data centers can be reformulated as follows:

$$\hat{C}_j^{iot} = \sum_{\tau \in \mathcal{T}} \{ \pi_{\tau} p_{j,\tau}^{iot} + \frac{H_{j,\tau}^{iot}}{V_{iot}} [S_{j,\tau}^{iot} - U_{j,\tau}^{iot,cal} - U_{j,\tau}^{iot,tran}] \} \quad (8a)$$

$$\begin{aligned} \hat{C}_j^{fdc} &= \sum_{\tau \in \mathcal{T}} \{ \pi_{\tau} p_{j,\tau}^{fdc} \\ &\quad + \frac{H_{j,\tau}^{fdc}}{V_{fdc}} [U_{j,\tau}^{iot,tran} - U_{j,\tau}^{fdc,cal} - U_{j,\tau}^{fdc,tran}] \}, \end{aligned} \quad (8b)$$

where V_{iot} and V_{fdc} are hyper-parameters helping balance the economic benefit and stability of queues. As the Lyapunov drift term becomes larger, the queue stability worsens. The objective function in (2t) and (2v) can be reformulated as (8a) and (8b). Since the second terms in (8a) and (8b) are bounded, under the assumption that optimal W-only policy exists, limiting constraints, i.e. (2i) and (2r), can be automatically guaranteed according to the Lyapunov optimization theory [45]. In this way, these limiting constraints are avoided. Since the reformulated objective function for the fog center as in (8a) and (8b), and time delay constraints for the M/M/1 queue as in (3d) contain bi-linear terms, the centralized synergy problem

is formulated as a mixed integer quadratically constrained quadratic programming (MIQCQP) as:

$$\begin{aligned} \min_{\mathbf{x}} \quad & \sum_{\tau \in \mathcal{T}} \left\{ \sum_{j \in \mathcal{N}_g} \kappa_{\tau} p_{j,\tau}^g + \sum_{j \in \mathcal{N}_{ess}} \pi_{\tau} (p_{j,\tau}^{cha} - p_{j,\tau}^{dis}) + \right. \\ & \left. \sum_{j \in \mathcal{N}_{cdc}} \pi_{\tau} p_{j,\tau}^{cdc} + \sum_{ij \in \mathcal{N}_b} r_{ij} l_{ij,\tau} \right\} + \sum_{j \in \mathcal{N}_{iot}} \hat{c}_j^{iot} + \sum_{j \in \mathcal{N}_{fdc}} \hat{c}_j^{fdc} \end{aligned} \quad (9a)$$

$$\text{s.t.} \quad (1a) - (1q), (2a) - (2h), \quad (9b)$$

$$(2j) - (2q), (2s) - (2w), (3a) - (3e). \quad (9c)$$

The constructed MIQCQP is computationally challenging to solve, even for state-of-the-art commercial solvers [46].

C. Reformulated Normalized Multi-parametric Disaggregation Technique

To overcome heavy computational issues of MIQCQP, we here introduce the novel reformulated normalized multi-parametric disaggregation technique (RNMDT) to transform the original non-convex problem into mixed integer non-linear programming (MINLP) at an arbitrary precision, which is crucial to ensure the convergence for the Lagrangian decomposition-based distributed optimization [46]. Take one term from (8a), i.e., $H_{j,\tau}^{iot} U_{j,\tau}^{iot,cal}$, for instance. It can be reformulated as follows:

$$\begin{aligned} H_{j,\tau}^{iot} U_{j,\tau}^{iot,cal} &= U_{j,\tau}^{iot,cal} H_{j,\tau}^l \\ &+ (H_{j,\tau}^u - H_{j,\tau}^l) \left(\sum_{e \in [\vartheta, -1]} 2^e \hat{y}_{j,e,\tau} + \Delta w_{j,\tau} \right) \end{aligned} \quad (10a)$$

$$H_{j,\tau}^{iot} = H_{j,\tau}^l + (H_{j,\tau}^u - H_{j,\tau}^l) \left(\sum_{e \in [\vartheta, -1]} 2^e z_{j,e,\tau}^{iot} + \Delta u_{j,\tau} \right) \quad (10b)$$

$$U_{j,\tau}^l z_{j,e,\tau}^{iot} \leq \hat{y}_{j,e,\tau} \leq U_{j,\tau}^u z_{j,e,\tau}^{iot} \quad (10c)$$

$$U_{j,\tau}^l (1 - z_{j,e,\tau}^{iot}) \leq U_{j,\tau}^{iot,cal} - \hat{y}_{j,e,\tau} \leq U_{j,\tau}^u (1 - z_{j,e,\tau}^{iot}) \quad (10d)$$

$$2^\vartheta (U_{j,\tau}^{iot,cal} - U_{j,\tau}^u) + U_{j,\tau}^u \Delta u_{j,\tau} \leq \Delta w_{j,\tau} \quad (10e)$$

$$\Delta w_{j,\tau} \leq 2^\vartheta (U_{j,\tau}^{iot,cal} - U_{j,\tau}^l) + U_{j,\tau}^l \Delta u_{j,\tau} \quad (10f)$$

$$U_{j,\tau}^l \Delta u_{j,\tau} \leq \Delta w_{j,\tau} \leq U_{j,\tau}^u \Delta u_{j,\tau} \quad (10g)$$

$$0 \leq \Delta u_{j,\tau} \leq 2^\vartheta, \vartheta \in \mathbb{Z}^-, \quad (10h)$$

where $z_{j,e,\tau}^{iot}$ is the binary variable. The reformulation can be made arbitrarily exact through employing a segment parameter ϑ . The variable $H_{j,\tau}^{iot}$ is discretized into $|\vartheta|$ parts, with the smallest size of 2^ϑ . This bisection method for discretizing the linear variable introduces less binary variables to reach the same precision as the classical McCormick envelopes [47], where the number of binary variables for RNMDT is $|\vartheta|$. This approach is applied to all the bi-linear terms in (8a) and (8b). The time delay model in (3d) is simplified as:

$$n_{j,\tau} I_j \leq (\mu_{j,\tau} n_{j,\tau} I_j - \lambda_{j,\tau}) \tau_{cdc}, \quad (11)$$

where $\mu_{j,\tau}$ is a linear variable and $n_{j,\tau}$ is a non-negative integer. The non-linear term, i.e., $\mu_{j,\tau} n_{j,\tau}$, is reformulated as:

$$\mu_{j,\tau} n_{j,\tau} = \sum_{e \in [1, k_1]} 2^{e-1} \hat{n}_e + (M_{j,cdc} - 2^{k_2-1} + 1) \hat{n}_e \quad (12a)$$

$$n_{j,\tau} = \sum_{e \in [1, k_1]} 2^{e-1} z_e^{cdc} + (M_{j,cdc} - 2^{k_2-1} + 1) z_e^{cdc} \quad (12b)$$

$$k_1 = \lfloor \log_2(M_{j,cdc} + 1) \rfloor \quad (12c)$$

$$k_2 = \lceil \log_2(M_{j,cdc} + 1) \rceil \quad (12d)$$

$$0 \leq \hat{n}_e \leq z_e^{cdc} \quad (12e)$$

$$0 \leq \mu_{j,\tau} - \hat{n}_e \leq 1 - z_e^{cdc}, \quad (12f)$$

where z_e^{cdc} is the binary variable. This reformation for the non-linear term with a non-negative integer is exact.

Let $\mathcal{J}(\mathbf{x})$ be the objective function of the reformulated problem by Lyapunov optimization, i.e., MIQCQP. Let $\sigma_\Omega(\mathbf{x})$ denotes the indicator function for the constraint set $\Omega(\mathbf{x})$, where $\sigma_\Omega(\mathbf{x}) = 0$ if $\mathbf{x} \in \Omega(\mathbf{x})$, and $\sigma_\Omega(\mathbf{x}) = +\infty$, otherwise. The problem (MIQCQP) can be represented by the infimum of an extended real-value function, i.e., $\mathcal{P}: \min \{ \mathcal{J}(\mathbf{x}) + \sigma_\Omega(\mathbf{x}) \}$. $\mathcal{P}_\vartheta: \min \{ \mathcal{J}_\vartheta(\mathbf{x}) + \sigma_{\Omega_\vartheta}(\mathbf{x}) \}$ can represent the relaxed form of \mathcal{P} via RNMDT with an arbitrary parameter $\vartheta, \vartheta < 0$.

Lemma 2: Assume $0 \in \text{int } \sigma_\Omega(\mathbf{x})$. Then the following optimality condition holds:

$$\inf_{\mathbf{x}} \mathcal{P}_\vartheta \xrightarrow{\vartheta \rightarrow -\infty} \inf_{\mathbf{x}} \mathcal{P}. \quad (13)$$

Proof: There are two cases for the relaxation.

Case 1: When one variable in the non-linear term is non-negative integer, the relaxation via RNMDT over the integer variable is exact. This case is employed for the time delay model as in the (12a)-(12f). The segment parameter ϑ is fixed as k_1 as in (12c), the McCormick envelope is simplified to be exact reformulations as in (12e) and (12f). For this case, the optimality condition (13) holds true for the fixed parameter ϑ .

Case 2: When two variables in the non-linear term are both linear, the relaxation of one of the variables via RNMDT can be made arbitrarily exact. This case is for the Lyapunov drift term as in (10a)-(10h). The linear variable $H_{j,\tau}^{iot}$ as in (10a)-(10h) is actually divided into two parts, i.e., an exact part for $\sum_{e \in [\vartheta, -1]} 2^e z_{j,e,\tau}^{iot}$ and an approximate part for $\Delta u_{j,\tau}$. The error of this relaxation is mainly introduced by the approximate part, i.e., $\Delta u_{j,\tau}$, which is upper bounded by 2^ϑ . This indicates that if the segmentation is large enough, i.e., $\vartheta \rightarrow -\infty$, the error introduced by the discretization method approaches zero. For arbitrary $\mathbf{x}^\dagger \in \Omega(\mathbf{x})$, the following relations can be obtained following [46], [48]:

$$e\text{-}\lim_{\vartheta \rightarrow -\infty} \sup (\mathcal{J}_\vartheta(\mathbf{x}^\dagger) + \sigma_{\Omega_\vartheta}(\mathbf{x}^\dagger)) \leq \mathcal{J}(\mathbf{x}^\dagger) + \sigma_\Omega(\mathbf{x}^\dagger) \quad (14a)$$

$$\mathcal{J}(\mathbf{x}^\dagger) + \sigma_\Omega(\mathbf{x}^\dagger) \leq e\text{-}\lim_{\vartheta \rightarrow -\infty} \inf (\mathcal{J}_\vartheta(\mathbf{x}^\dagger) + \sigma_{\Omega_\vartheta}(\mathbf{x}^\dagger)). \quad (14b)$$

These relations further imply that a sequence of relaxed problems, $\{\mathcal{P}_\vartheta\}_{\vartheta=-1}^\infty$, epi-converges uniformly to the original problem \mathcal{P} when $\vartheta \rightarrow -\infty$ as follows:

$$\{\mathcal{J}_\vartheta(\mathbf{x}) + \sigma_{\Omega_\vartheta}(\mathbf{x})\}_{\vartheta=-1}^\infty \xrightarrow[\text{epi-converge}]{} \mathcal{J}(\mathbf{x}) + \sigma_\Omega(\mathbf{x}). \quad (15)$$

Assume that functions $\mathcal{J}_\vartheta(\mathbf{x}) + \sigma_{\Omega_\vartheta}(\mathbf{x})$ and $\mathcal{J}(\mathbf{x}) + \sigma_\Omega(\mathbf{x})$ are both proper and lower semi-continuous, where $\mathcal{J}(\mathbf{x}) + \sigma_\Omega(\mathbf{x})$ is bounded below on bounded sets and $\mathcal{J}_\vartheta(\mathbf{x}) + \sigma_{\Omega_\vartheta}(\mathbf{x})$ is equi-hypercoercive as follow:

$$\lim_{\mathbf{x} \rightarrow \infty} \frac{\mathcal{J}_\vartheta(\mathbf{x}) + \sigma_{\Omega_\vartheta}(\mathbf{x})}{\|\mathbf{x}\|_1} = +\infty. \quad (16)$$

Equation (16) can be satisfied due to the quadratic terms in the objective function $\mathcal{J}_\theta(\mathbf{x})$. Allied with the premise of $0 \in \text{int } \sigma_\Omega(\mathbf{x})$, the optimality condition (13) can be obtained [49].

III. PRIVACY-PRESERVING DISTRIBUTED APPROACH

The reformulated small-scale MINLP for the co-dispatch of data center penetrated power networks can be solved by the mature commercial solvers. However, this optimization problem is spatially and temporally correlated. When the scalability of the problem increases, the commercial software has the problem of deriving optimal solutions within finite time due to the curse of dimension introduced by integer variables. Meanwhile, the centralized method infringes on the privacy of different entities in the integrated system. To deal with these issues, we propose the distributed privacy-preserving optimization approach to solve the non-convex and non-smooth problem. Meanwhile, it can also help to mitigate the computational burden for large-scale problem by exploiting the property of exponential reduction of complexity through decoupling spatial correlations and coordinating the sharing of a sequence of decision variables for the distributed computation.

A. General Formulation of the Co-Dispatch Problem

For easy decomposition, we can rewrite the problem into a compact form as follows:

$$\min_{\mathbf{x}} \quad \mathcal{J}(\mathbf{x}) = \sum_{i \in \mathcal{D}} \sum_{\tau \in \mathcal{T}} \mathcal{J}_{i,\tau}(\mathbf{x}_{i,\tau}) \quad (17a)$$

$$\text{s.t.} \quad \mathbf{x}_{i,\tau} \in \mathcal{X}_i, \forall i \in \mathcal{D} \quad (17b)$$

$$\varpi_{i,p}\mathbf{x}_{i,\tau} = \varpi_{i',p}\mathbf{x}_{i',\tau}, \forall i \in \mathcal{N}_p, i' \in \mathcal{D}/\mathcal{N}_p \quad (17c)$$

$$\varpi_{i,d}\mathbf{x}_{i,\tau} = \varpi_{i',d}\mathbf{x}_{i',\tau}, \forall i \in \mathcal{N}_{iot,(fdc)}, i' \in \mathcal{N}_{fdc,(cdc)}, \quad (17d)$$

where the set \mathcal{D} is the collection of agents in integrated power systems, i.e., $\mathcal{D} = \mathcal{N}_p \cup \mathcal{N}_{ess} \cup \mathcal{N}_{gen} \cup \mathcal{N}_{iot} \cup \mathcal{N}_{fdc} \cup \mathcal{N}_{cdc}$. Vector $\mathbf{x}_{i,\tau}$ contains the decision variables for each entity i at each time step τ . \mathcal{X}_i forms the non-convex feasible region for the decision variable, constructed by the mixed integer non-linear constraints (1b)-(1q), (2a)-(2w), (3a)-(3e), (10a)-(10h), (12a)-(12f). $\varpi_{i,p}$ and $\varpi_{i,d}$ are the mapping matrices for the energy and communication coupling constraints:

$$\varpi_{i,p}\mathbf{x}_{i,\tau} = (p_{i,\tau}^g, p_{i,\tau}^{iot}, p_{i,\tau}^{fdc}, p_{i,\tau}^{cdc}, p_{i,\tau}^{dis} - p_{i,\tau}^{cha})^T, \forall i \in \mathcal{N}_p \quad (18a)$$

$$\varpi_{i,d}\mathbf{x}_{i,\tau} = (U_{i,\tau}^{iot,tran}, U_{i,\tau}^{fdc,tran})^T, \forall i \in \mathcal{N}_{iot}/\mathcal{N}_{fdc}. \quad (18b)$$

The reformulated optimization problem is a MINLP. To overcome the non-smoothness of the problem, the ℓ_1 -surrogate Lagrangian relaxation method is proposed to solve the problem in a distributed privacy-preserving manner.

$$\begin{aligned} \min_{\mathbf{x}} \quad & \mathcal{L}_\eta(\mathbf{x}_i, \mathbf{x}_{i'}, \zeta_{i,p}, \zeta_{i,d}) = \sum_{i \in \mathcal{D}} \sum_{\tau \in \mathcal{T}} \{\mathcal{J}_{i,\tau}(\mathbf{x}_{i,\tau})\} \\ & + \sum_{i \in \mathcal{N}_p, i' \in \mathcal{D}/\mathcal{N}_p} \sum_{\tau \in \mathcal{T}} \{\zeta_{i,\tau,p}(\varpi_{i,p}\mathbf{x}_{i,\tau} - \varpi_{i',p}\mathbf{x}_{i',\tau}) \\ & + \eta_p \|\varpi_{i,p}\mathbf{x}_{i,\tau} - \varpi_{i',p}\mathbf{x}_{i',\tau}\|_1\} \end{aligned}$$

$$\begin{aligned} & + \sum_{\substack{i \in \mathcal{N}_{iot,(fdc)} \\ i' \in \mathcal{N}_{fdc,(cdc)}}} \sum_{\tau \in \mathcal{T}} \{\zeta_{i,\tau,d}(\varpi_{i,d}\mathbf{x}_{i,\tau} - \varpi_{i',d}\mathbf{x}_{i',\tau}) \\ & + \eta_d \|\varpi_{i,d}\mathbf{x}_{i,\tau} - \varpi_{i',d}\mathbf{x}_{i',\tau}\|_1\} \end{aligned} \quad (19a)$$

$$\text{s.t.} \quad \mathbf{x}_{i,\tau}, \mathbf{x}_{i',\tau} \in \mathcal{X}_i, \forall i, i' \in \mathcal{D}, \quad (19b)$$

where the global equality constraints (18a) and (18b) are penalized through the ℓ_1 -norm, helping boost convergence of the distributed optimization. To further increase smoothness of the augmented Lagrangian problem, the ℓ_1 -norm can be reformulated through a set of inequality constraints, we refer interesting readers to [29], [50] for more details.

Algorithm 1 Customized Distributed ℓ_1 -Surrogate Lagrangian Decomposition Algorithm.

```

Initialize  $\mathbf{x}_{i,\tau}^0, \mathbf{x}_{i',\tau}^0, \zeta_{i,\tau,p}^0, \zeta_{i,\tau,d}^0, \eta_p^0, \eta_d^0, K_{max}, \epsilon$ 
For each iteration  $k = 0, 1, 2, \dots, K_{max}$  do
  For each agent  $i, i' \in \mathcal{D}$  do
    Receive variables  $\mathbf{x}_{i',\tau}^k$  from other agents
    Solve the decomposed sub-problem in (19a)-(19b)
    Check surrogate optimality condition in (21a) and (21b)
    If the surrogate optimality condition is satisfied:
      Update dual variables following (22a) and (22b)
    else
      Update dual variables as  $\zeta_{i,\tau,p}^{k+1} = \zeta_{i,\tau,p}^k, \zeta_{i,\tau,d}^{k+1} = \zeta_{i,\tau,d}^k$ 
    end if
    Share variables  $\mathbf{x}_{i,\tau}^{k+1}$  to other agents
  end for
  Update penalty terms following (26a) and (26b)
  Check residuals defined in (24) and (27)
end for

```

B. Customized Distributed Privacy-Preserving Approach

We can define the decomposed sub-problem for each entity at each iteration. Take the sub-problem for the power network operator, i.e., $i \in \mathcal{N}_p$, for instance. It can be formulated as:

$$\begin{aligned} \min_{\mathbf{x}_{i,\tau}} \quad & \mathcal{L}_{\eta,i}(\mathbf{x}_i, \mathbf{x}_{i'}, \zeta_{i,p}, \zeta_{i,d}) = \sum_{\tau \in \mathcal{T}} \{\mathcal{J}_{i,\tau}(\mathbf{x}_{i,\tau}) \\ & + \zeta_{i,\tau,p} \varpi_{i,p}\mathbf{x}_{i,\tau} + \eta_p \|\varpi_{i,p}\mathbf{x}_{i,\tau} - \varpi_{i',p}\mathbf{x}_{i',\tau}\|_1\} \end{aligned} \quad (20a)$$

$$\text{s.t.} \quad \mathbf{x}_{i,\tau}, \mathbf{x}_{i',\tau} \in \mathcal{X}_i, \forall i \in \mathcal{N}_p, i' \in \mathcal{D}/\mathcal{N}_p, \quad (20b)$$

where the power network operator is responsible for calculating the optimal power flow and ensuring the energy power conservation. The fourth and fifth terms in (19a) are not included for the power network, but will take effects for the IoT edge, fog, or cloud data centers, i.e., $i \in \mathcal{N}_{iot}/\mathcal{N}_{fog}/\mathcal{N}_{cdc}$.

To overcome non-smoothness and facilitate convergence of the optimization problem, the surrogate optimality condition can be defined for agent $i, i \in \mathcal{D}$, at iteration k as follows:

$$\mathcal{L}_\eta(\mathbf{x}_i^{k+1}, \mathbf{x}_{i'}^k, \zeta_{i,p}^k, \zeta_{i,d}^k) \leq \mathcal{L}_\eta(\mathbf{x}_i^k, \mathbf{x}_{i'}^k, \zeta_{i,p}^k, \zeta_{i,d}^k) \quad (21a)$$

$$\mathcal{L}_\eta(\mathbf{x}_i^k, \mathbf{x}_{i'}^{k+1}, \zeta_{i,p}^k, \zeta_{i,d}^k) \leq \mathcal{L}_\eta(\mathbf{x}_i^k, \mathbf{x}_{i'}^k, \zeta_{i,p}^k, \zeta_{i,d}^k). \quad (21b)$$

If the surrogate optimality condition is satisfied, the line search on the sub-gradient direction forms acute angles towards optimal dual variables. Dual variables will be updated as:

$$\zeta_{i,\tau,p}^{k+1} = \zeta_{i,\tau,p}^k + \xi^k (\varpi_{i,p}\mathbf{x}_{i,\tau}^{k+1} - \varpi_{i',p}\mathbf{x}_{i',\tau}^k) \quad (22a)$$

$$\zeta_{i,\tau,d}^{k+1} = \zeta_{i,\tau,d}^k + \xi^k (\varpi_{i,d} \mathbf{x}_{i,\tau}^{k+1} - \varpi_{i',d} \mathbf{x}_{i',\tau}^k). \quad (22b)$$

The stepsize toward the surrogate direction should be appropriately decided to ensure the convergence of the problem. The Polyak step-size rule is leveraged following [29] as:

$$\xi^k = \alpha_k \frac{\|\gamma_p^{k-1}\|_2}{\|\gamma_p^k\|_2}, \quad (23)$$

where γ_p^k represents the primal residual at iteration k :

$$\begin{aligned} \gamma_p^k = & \sum_{i \in \mathcal{N}_p, i' \in \mathcal{D}/\mathcal{N}_p} \sum_{\tau \in \mathcal{T}} (\varpi_{i,p} \mathbf{x}_{i,\tau}^k - \varpi_{i',p} \mathbf{x}_{i',\tau}^k) \\ & + \sum_{i \in \mathcal{N}_{iot,(fdc)}} \sum_{\tau \in \mathcal{T}} (\varpi_{i,d} \mathbf{x}_{i,\tau}^k - \varpi_{i',d} \mathbf{x}_{i',\tau}^k), \end{aligned} \quad (24)$$

$i', i' \in \mathcal{N}_{fdc,(cdc)}$

where the ancillary parameter α_k is updated as follow:

$$\alpha_k = 1 - \frac{1}{c^k \theta}, \quad \theta = 1 - \frac{1}{k^r} \quad (25a)$$

$$c \geq 1, \quad 0 < r < 1. \quad (25b)$$

The penalty term is updated adaptively following:

$$\eta_{p(d)}^{k+1} = \eta_{p(d)}^k / w, \quad (21a) \text{ or } (21a) \text{ is not satisfied} \quad (26a)$$

$$\eta_{p(d)}^{k+1} = \eta_{p(d)}^k \cdot w, \quad \text{Otherwise.} \quad (26b)$$

Define the dual residual at iteration k as:

$$\begin{aligned} \gamma_d^k = & \sum_{i' \in \mathcal{D}/\mathcal{N}_p} \sum_{\tau \in \mathcal{T}} (\varpi_{i,p} \mathbf{x}_{i,\tau}^k - \varpi_{i',p} \mathbf{x}_{i',\tau}^{k-1}) \\ & + \sum_{i' \in \mathcal{N}_{fdc,(cdc)}} \sum_{\tau \in \mathcal{T}} (\varpi_{i,d} \mathbf{x}_{i,\tau}^k - \varpi_{i',d} \mathbf{x}_{i',\tau}^{k-1}), \quad k > 0. \end{aligned} \quad (27)$$

At each iteration k , each agent in the system is responsible to send and receive data with other agents as required in Algorithm 1. Specifically, as illustrated in Fig. 3, IoT data center, fog data center, and cloud data center need to interact with each other by sharing variables sequentially to keep communication conservation, i.e., the amount of incoming tasks should equal the amount of processed, transmitted, and stored tasks. These shared variables include $U_{i/i',\tau}^{iot,tran,k}$ and $U_{i/i',\tau}^{fdc,tran,k}$. Meanwhile, generator, ESS, allied with edge-fog-cloud data centers, must coordinate with the power network operator to keep energy conservation by exchanging active power consumption variables, i.e., $p_{i/i',\tau}^{g,k}, p_{i/i',\tau}^{iot,k}, p_{i/i',\tau}^{fdc,k}, p_{i/i',\tau}^{cdc,k}, p_{i/i',\tau}^{dis,k} - p_{i/i',\tau}^{cha,k}$. Moreover, to ensure the convergence, each agent needs to interact with the power network operator by sharing personal augmented Lagrangian function value, i.e., $\mathcal{L}_{\eta,i}^k$, and receiving the overall Lagrangian function value, i.e., \mathcal{L}_{η}^k , for deciding the satisfaction of surrogate Lagrangian conditions. If the primal and dual residuals are below the stopping criteria, the distributed algorithm will be terminated. We analyze the asymptotic complexity for the proposed distributed privacy-preserving algorithm using the \mathcal{O} notation. Suppose there are total N agents in the system. In each iteration, each agent transmits its own local variables from the d -dimensional set, i.e., $U_{i,\tau}^{iot,tran,k}, U_{i,\tau}^{fdc,tran,k}, p_{i,\tau}^{g,k}, p_{i,\tau}^{iot,k}, p_{i,\tau}^{fdc,k}, p_{i,\tau}^{cdc,k}, p_{i,\tau}^{dis,k} - p_{i,\tau}^{cha,k}$ and $\mathcal{L}_{\eta,i}^k$, to the power network operator or to its neighbors, which may include IoT edge centers, fog data

centers, or cloud data centers. In return, the power network operator or its neighbors send back the updated shared or global variables from the d -dimensional set, i.e., $U_{i',\tau}^{iot,tran,k}, U_{i',\tau}^{fdc,tran,k}, p_{i',\tau}^{g,k}, p_{i',\tau}^{iot,k}, p_{i',\tau}^{fdc,k}, p_{i',\tau}^{cdc,k}, p_{i',\tau}^{dis,k} - p_{i',\tau}^{cha,k}$ and \mathcal{L}_{η}^k . In the uplink phase, each agent sends at most a d -dimensional vector. In the downlink phase, each agent receives at most a d -dimensional vector. Therefore, communication cost per iteration per agent is $\mathcal{O}(d)$. Across N agents, the communication cost per iteration for the system is $\mathcal{O}(Nd)$. Assuming the algorithm takes K iterations to converge, the total asymptotic communication complexity is $\mathcal{O}(NdK)$. The asymptotic communication complexity depends on the dimension of the shared variables, the number of agents, and the number of iterations required for convergence.

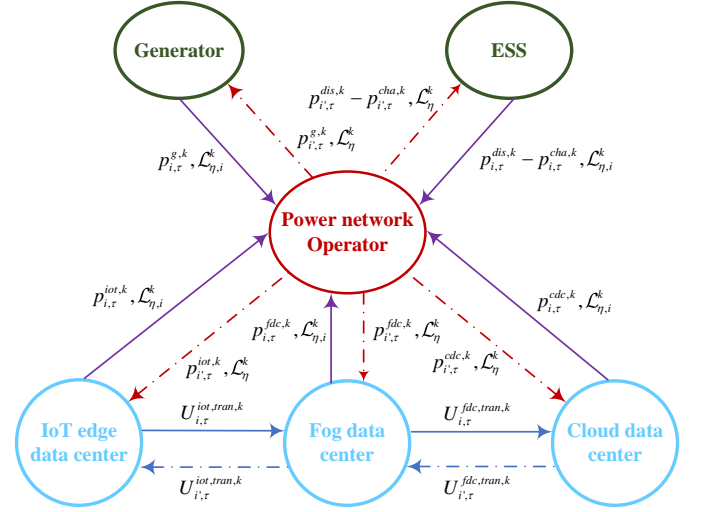


Fig. 3. Variable sharing in distributed privacy-preserving computing.

C. Convergence Analysis

Proposition 1: With parameter settings in (25a)-(25b) and (26a)-(26b), Algorithm 1 can ensure that the ℓ_1 -Lagrangian relaxed problem converges to optimal solutions of \mathcal{P}_ϑ , and ultimately epi-converges to optimal solutions of \mathcal{P} .

Proof: When surrogate optimality conditions, i.e, (21a) and (21b), are met, the ℓ_1 -surrogate Lagrangian relaxed problem can converge to the optimal solutions [50]. Conversely, when surrogate optimality conditions are not met over iterations, penalty factors $\eta_{p(d)}^k$ decrease and finally tend to zero. Convergence for the optimization problem under this situation can be theoretically guaranteed with the parameter settings in (25a)-(25b), and (26a)-(26b) following [29]. Meanwhile, the ℓ_1 -surrogate Lagrangian method can converge to optimal solutions with a linear convergence rate. From [50], [51], the relation between dual variables and surrogate Lagrangian function value can be constructed as:

$$\begin{aligned} & \beta \cdot \|\eta_{p(d)}^* - \eta_{p(d)}^k\|^2 \\ & \leq \mathcal{L}_{\eta}^*(\mathbf{x}_i, \mathbf{x}_{i'}, \zeta_{i,p}, \zeta_{i,d}) - \mathcal{L}_{\eta}(\mathbf{x}_i, \mathbf{x}_{i'}, \zeta_{i,p}, \zeta_{i,d}), \end{aligned} \quad (28)$$

where $\eta_{p(d)}^*$ and $\mathcal{L}_{\eta}^*(\mathbf{x}_i, \mathbf{x}_{i'}, \zeta_{i,p}, \zeta_{i,d})$ refer to the optimal dual variables and Lagrangian function value, respectively. Thus, the parameter β exists, which satisfies the condition

that $0 < \beta < \frac{1}{2\xi^k}$. The distance between dual variables and their optimal values is proportional to the violation of global constraints. Dual variables $\eta_{p(d)}^k$ can converge the optimal values with an approximate linear rate of $\sqrt{1 - 2\beta\xi^k} < 1$ outside a sphere centered at $\eta_{p(d)}^*$. Recall Lemma 2, the optimality condition in (13) holds true when the parameter ϑ is made arbitrarily small. This implies that the optimal solutions of the relaxed MINLP problem epi-converge to those of the original MIQCQP problem. Overall, by leveraging the surrogate optimality conditions and adaptively adjusted stepsizes, the proposed approach is theoretically guaranteed to yield optimal solutions the original problem \mathcal{P} as the parameter ϑ is sufficiently small. Furthermore, we verify the effectiveness and convergence of the proposed approach via the numerical simulations.

IV. NUMERICAL SIMULATIONS

A. Simulation Setup

The code is implemented in Matlab 2020 on a computer with 6-core Intel i5-10500 CPU@3.10GH, and the state-of-the-art commercial solver, Gurobi 11.0, is employed to solve the centralized problem and decomposed sub-problems. The standard IEEE 15-bus, 33-bus, and 85-bus distribution systems [52] penetrated with data centers are adopted to verify the optimality and efficiency of the proposed distributed privacy-preserving approach. The day-ahead real PV and wind power generation data are derived from [53], and the communication traffic data are adopted from [54]. Day-ahead locational marginal prices are derived from the UK electricity market [55]. The load task requests at the IoT data center j , i.e., $S_{j,\tau}^{iot}$, are randomly generated from the Poisson distribution [56]. These data used in this paper are available in the public repository [57]. The real-time time-slot is set to be the same as dispatch time-slot for simplicity in this paper. Parameters for updating step size are set as: $c = 200$, $r = \frac{1}{\sqrt{k}}$, and $w = 1.01$.

B. IEEE 15-Bus Systems with Simplified Data Centers

The synergy of hierarchical data centers and power networks constitutes a non-convex and non-smooth optimization problem, posing significant challenges in obtaining near-optimal solutions, even with centralized methods. To validate the near-optimality of the proposed distributed privacy-preserving approach, a case study is thus designed using the simplified data center structure with lower complexity. Specifically, The optimality and convergence of the proposed distributed approach are first verified on the IEEE 15-bus systems with simplified data centers. The stopping criteria for primal and dual residuals are set as $\gamma_p^k \leq 10^{-2}$ and $\gamma_d^k \leq 10^{-2}$ or $|\gamma_p^{k+1} - \gamma_p^k| \leq 10^{-6}$. The initial step size is set to 1.3. As illustrated in Fig. 4, the traditional diesel generator is positioned at bus 1, with a fog data center located at bus 10. Additionally, a cloud data center is placed at bus 3 together with the combined renewable energy generators (wind and power generators). The effectiveness of RNMDT method is verified under both the centralized and distributed settings with different segment parameter ϑ . When $\vartheta = 0$, the RNMDT

method becomes a set of classical McCormick envelopes [47], which represents the loosest approximation. As denoted in Table I, the original optimization problem contains 216 binary variables, with additional 48 quadratic terms in the objective function (48o) and 336 quadratic terms in constraints (336c). The original optimization problem is a non-convex MIQCQP. Through approximation by RNMDT with slightly increased binary variables, the quadratic terms in the objective function are removed, left with quadratic constraints, i.e., convex second-order cone constraints denoted by (1e). As in Table II, the classical McCormick envelope method, i.e., $\vartheta = 0$, obtains a lower cost than the optimal solution. As the segment parameter decreases, solutions obtained by the RNMDT tend to the optimal one. Meanwhile, the relaxed problem by the RNMDT requires much lower computational costs than the original problem.

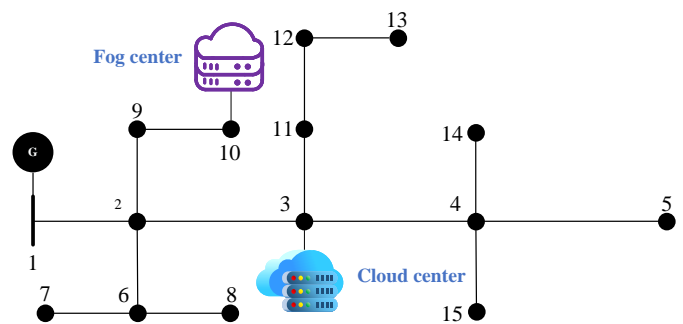


Fig. 4. IEEE 15-bus system with simplified data centers.

As illustrated in Fig. 5 (a), the primal and dual residuals drop to the stopping criteria around 49 iterations when $\vartheta = -3$. As in Fig. 5 (b), the adaptive mechanism for penalty term contributes to the further decrease of surrogate Lagrangian function value. With the decrement of segment parameter under the distributed setting, solutions obtained by the RNMDT tend to the optimal one as in Table III. Meanwhile, the original problem solved directly in the distributed manner obtains the solution with higher gaps due to its inherent high non-convexities introduced by the quadratic terms. These results illustrate the exactness and effectiveness of relaxing quadratic terms through RNMDT. Moreover, the exactness of the SOCP relaxation is verified. At each dispatch time slot, the largest errors, i.e., the error from equation (1e), for all buses are obtained. As illustrated in the Fig. 6, the relaxation is shown to be exact, with the largest errors across all buses at each dispatch time slot being negligible.

TABLE I
STATISTICS OF MODEL PARAMETERS FOR 15-BUS SYSTEM

	Binary Variables	Continuous Variables	Quadratic Terms
Original	216	4896	48o+336c
0	216	2978	336c
-1	217	2989	336c
-3	230	3027	336c
-12	504	5856	336c

TABLE II
CENTRALIZED METHOD USING DIFFERENT PARAMETERS

	Original	0	-1	-3	-12
Value	12468.31	12462.92	12468.31	12468.31	12468.31
Time (s)	4.68	3.51	3.80	3.93	7.26

Figure 5 consists of two subplots. Subplot (a) shows the primal and dual residuals on a logarithmic scale from 10^{-2} to 10^0 over 50 iterations. Both residuals decrease rapidly and converge to approximately 10^{-2} by iteration 40. Subplot (b) shows the surrogate value (blue line) and the penalty term (red dashed line) over 50 iterations. The surrogate value decreases from 1.7×10^4 to 1.2×10^4 , while the penalty term increases from 180 to 300.

Fig. 5. Convergence curves. (a) primal and dual residuals. (b) evolution of the surrogate value and penalty term.

TABLE III
DISTRIBUTED METHOD USING DIFFERENT PARAMETERS

	Original	0	-1	-3	-12
Value	12465.56	12460.72	12466.33	12467.62	12467.61
Time (s)	267.40	252.65	253.07	273.03	288.24
Iteration	47	47	46	49	50

Figure 6 shows the error of SOCP relaxation over 24 hours. The error (p.u.) is plotted on a scale from 0 to 12. The error fluctuates significantly, with peaks reaching up to 12 p.u. around 10 and 15 hours.

Fig. 6. Error for the SOCP relaxation.

To further demonstrate the optimality of the proposed distributed approach (M3), we further compare it with the centralized method (M1) and the classic ADMM (M2) [58]. Define the relative absolute error as $|O_{M1} - O_{M2/M3}|/O_{M1} \cdot 100\%$, where O_{M1} , O_{M2} , and O_{M3} denote the optimal objective values obtained by M1, M2 and M3, respectively. For the distributed approach, the whole optimization problem is decomposed into a set of sub-problems for each agent, i.e., the power network operator, fog data center (FDC), cloud data center (CDC), and power plant generator. Each agent solves its own decomposed sub-problem and simultaneously shares limited data with other agents, which preserves privacy of personal data for each agent. As in Table IV, when $\vartheta = -3$, relative absolute errors for all the sub-problems are below 1%. Meanwhile, M3 obtains a solution with the overall error of 0.006% compared to the optimal solutions obtained from M1, which demonstrates that M3 can derive high-quality solutions for non-convex problem in a privacy-preserving manner. For the classic ADMM, i.e., M2, all the parameter settings are

kept the same as M3 except for the step-size. The step-size for M2 employed the initial step-size for M3, and we set the 200 iteration as the maximum limit. From the simulation results, M2 actually obtains a relatively large primal error, i.e., $\gamma_p^k > 10^{-1}$, within the maximum limits. For M2, the total relative error with regarding to the optimal objective function derived by M1 is 0.367%, with the relative error of 9.41% for the power network and the relative error of 7.69% for the generator. These simulation results demonstrate the superiority of the proposed distributed approach, i.e., M3, over the traditional distributed optimization method, i.e., M2.

TABLE IV
COSTS OF DIFFERENT ALGORITHMS (EUR)

	FDC	CDC	Generator	Power network	Total
M1	11023.94	815.42	614.07	14.88	12468.31
M2	11030.34	811.85	566.85	13.48	12422.52
M3	11030.34	811.80	610.63	14.85	12467.62
Error (M2)	0.06%	0.44%	7.69%	9.41%	0.367%
Error (M3)	0.06%	0.44%	0.56%	0.20%	0.006%

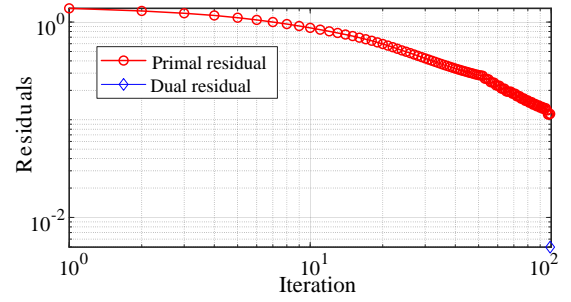


Fig. 7. Convergence curve for ADMM.

As in Fig. 9, incoming tasks at the fog data center are allocated to be either resolved locally at the fog data center, or stored in the data queue, or transferred remotely to cloud data center for computations to reach the minimum operational cost for the integrated systems. As illustrated in Fig. 10 (a), to meet the quality of services, the cloud data center should reserve adequate computing resources for the random incoming task requests from fog data center. Meanwhile, the cloud data center will priorly utilize the local renewable energy generations to perform computations for the incoming requests, and the diesel generator will coordinate with uncertain renewable energy generations to supply stable electricity for the whole system as illustrated in Fig. 10 (b). Specifically, The computational load is optimally scheduled based on the incoming task requests, hourly price signals, volume of the data queues, and the availability of renewable energy generation with zero marginal costs. As shown in Fig. 10 (b), renewable generation from the 1st to 5th hours is relatively low compared to other time periods. However, as illustrated in Fig. 8, the price signals during these hours are low, and the incoming tasks at the fog data centers are also low as depicted by the solid black line in Fig. 9. In this scenario, the traditional thermal generator is scheduled to supply sufficient power due to the low electricity prices, allowing a large portion of the computational load to be processed by the fog and data centers. Meanwhile,

during the 10th and 20th hours, with high price signals and abundant renewable energy generation, the traditional thermal generator is less scheduled to supply power, resulting in a balanced overall power supply. Despite the relatively high volume of incoming task requests during these hours, a portion of the requests is stored in the data queue for later processing, balancing the computational load effectively.

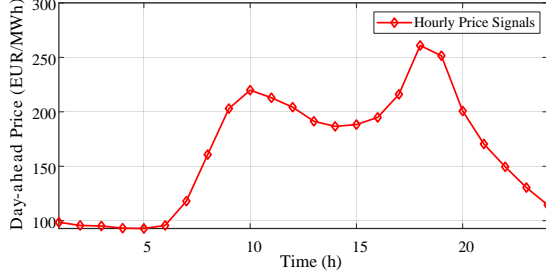


Fig. 8. Day-ahead price signals.

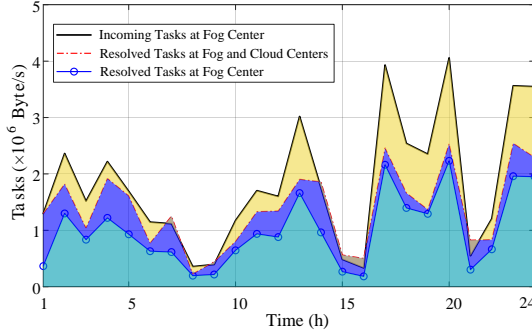


Fig. 9. Task allocations between fog and cloud centers.

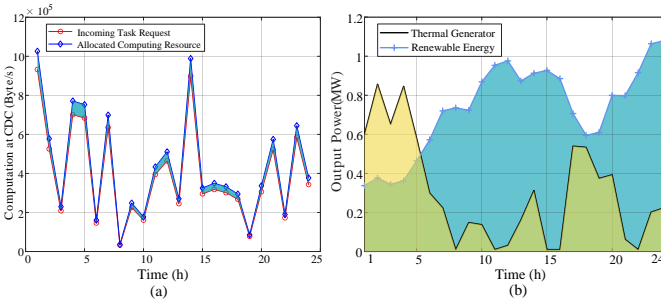


Fig. 10. Evolution of task demands and energy generations. (a) resource allocation at cloud data center (b) power supplies

C. IEEE 33-Bus Systems with Hierarchical Data Centers

The effectiveness and scalability of the proposed distributed approach are further verified on the IEEE 33-bus systems with hierarchical data centers. As illustrated in Fig. 11, the energy storage system (ESS) is deployed at bus 5. An edge data center is positioned at bus 16, together with the fog data center at bus 12 and cloud data center at bus 6, forming the three-tier hierarchical data centers. Due to the existence of additional ESS and edge data center, number of quadratic terms in the objective function and integer variables increases as given in

Table V, complicating the optimization problem. The stopping criteria for primal and dual residuals are set as $\gamma_p^k \leq 10^{-6}$ and $\gamma_d^k \leq 10^{-6}$ or $|\gamma_p^{k+1} - \gamma_p^k| \leq 10^{-6}$ for better performance of the distributed approach, and the initial step size is set to 1.3.

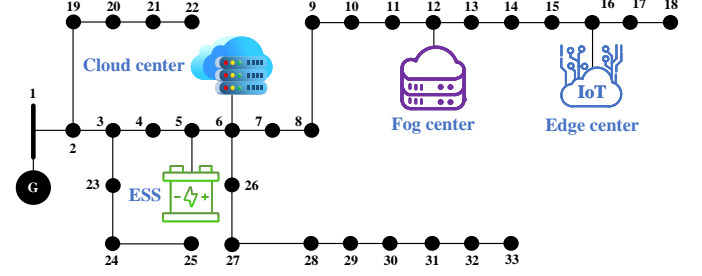


Fig. 11. IEEE 33-bus system with hierarchical data centers.

TABLE V
STATISTICS OF MODEL PARAMETERS FOR 33-BUS SYSTEM

	Binary Variables	Continuous Variables	Quadratic Terms
Original	240	12217	144o+768c
0	240	6470	768c
-5	456	7043	768c
-8	594	7388	768c
-12	785	7866	768c

TABLE VI
CENTRALIZED METHOD USING DIFFERENT PARAMETERS

	Original	0	-5	-8	-12
Value	-2575.43	-15243.73	-2595.88	-2789.21	-2509.52
Gap	144.77%	0.00%	72.12%	76.10%	63.14%
Time (s)	36000.00	48.85	36000.00	36000.00	36000.00

Since the objective function contains the Lyapunov drift terms, the combined equivalent operational cost can be negative. As denoted in Table VI, when $\vartheta = 0$, the classical McCormick envelope method obtains an optimal solution within 48.85s. However, the obtained value is far from the global optimal value due to the highly loose relaxation by the classical McCormick envelope method. Without relaxation by RNMDT, the centralized manner cannot derive the optimal solution within finite time, i.e., 10 hours, and the optimality gap is nearly 144.78%. RNMDT can facilitate the derivation of optimal solutions, while the optimality gap for all cases still remains high (over 63%), which is unacceptable for solving the day-ahead dispatch problem. Simulation results demonstrate that the traditional centralized method combined with efficient relaxations still cannot be leveraged to derive high-quality solutions for the complex synergy problem of hierarchical data centers penetrated power network. To deal with this challenge and meanwhile preserve privacy for agents in the integrated system, the efficiency of distributed ℓ_1 -surrogate Lagrangian method combined with RNMDT is further verified.

For the distributed setting, the whole optimization problem is decomposed into sub-problems for each agent, i.e., the power network operator, IoT edge data center (EDC), energy storage system (ESS), FDC, CDC, and power plant

TABLE VII
DISTRIBUTED METHOD USING DIFFERENT PARAMETERS

	Original	0	-5	-8	-12
Value	-	-15103.24	-2515.52	-2433.30	-2433.47
Iteration	-	149	162	182	170
Time ₁ (s)	-	1784.96	4935.27	5983.04	6669.85
Time ₂ (s)	-	297.49	822.55	997.17	1111.64

Figure 12 consists of two subplots. Subplot (a) shows the primal residual (red line with circles) and dual residual (blue line with circles) on a logarithmic scale from 10^0 to 10^{-8} against iterations from 10^0 to 10^2 . Both residuals decrease rapidly and then level off. Subplot (b) shows the surrogate value (blue line) and penalty term (red dashed line) against iterations from 0 to 150. The surrogate value decreases from 2000 to approximately -2500, while the penalty term increases from 0 to approximately 700.

Fig. 12. Convergence curves. (a) primal and dual residuals. (b) evolution of the surrogate value and penalty term.

generator. As denoted in Table VII, the proposed distributed privacy-preserving approach is verified with different segment parameter ϑ . Time₁ refers to the overall total time costs for deriving solutions for all agents, while Time₂ refers to the ideal agent-based average time in the distributed computation scenario. However, the surrogate Lagrangian method cannot work for the original optimization problem (without relaxation for the quadratic terms). With the decrement of parameter ϑ , the distributed algorithm can converge to the stable near-optimal solutions. Specifically, when $\vartheta = -8$, the distributed algorithm can converge to the required criteria within 182 iterations and 5984s (ideally 16.62 minutes for each agent in the distributed setting). As illustrated in Fig. 12 (a) and 12 (b), the surrogate optimality condition for this case is always satisfied and the penalty factors are incremented, contributing

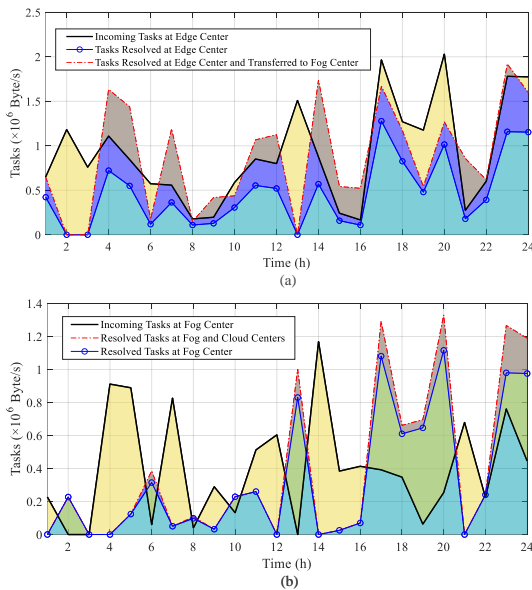


Fig. 13. Task allocations. (a) between edge and fog centers. (b) between fog and cloud centers.

to the convergence of distributed algorithm. Dispatch results for the three-tier hierarchical data centers are exhibited. As illustrated in Fig. 13 (a), incoming tasks at EDC are mostly resolved locally, which is denoted by the area enclosed by the solid blue circled line and x-axis. Beyond being stored in the data queue, partial tasks are also transferred to the fog data center for processing, as denoted by the area enclosed by the dash read line and solid blue circled line. For fog data center, as illustrated in Fig. 13 (b), incoming tasks from the EDC are also optimally allocated (to be either processed locally, stored in the data queue, or transferred to the cloud data center), to reach the optimal energy efficiency for the whole system.

D. IEEE 85-Bus Systems with Hierarchical Data Centers

The effectiveness and scalability of the proposed distributed approach are also verified on the large-scale IEEE 85-bus systems with hierarchical data centers. The power network topology for the IEEE 85-bus system is available in [52], where the location of each entity is given in Table VIII. Compared to the 15-bus and 33-bus cases with the same settings, this case contains more continuous and binary variables, as well as more quadratic terms in the constraints as illustrated in Table IX. For this case, the stopping criteria for primal and dual residuals are set the same as the 15-bus case, i.e., $\gamma_p^k \leq 10^{-2}$ and $\gamma_d^k \leq 10^{-2}$ or $|\gamma_p^{k+1} - \gamma_p^k| \leq 10^{-6}$. The initial step size is set to 1.3.

TABLE VIII
LOCATION OF ENTITIES IN THE 85-BUS SYSTEM

	Thermal generator	Renewable	Edge center	FDC	CDC	ESS
Bus	1	50	74	40	50	15

TABLE IX
STATISTICS OF MODEL PARAMETERS FOR 85-BUS SYSTEM

	Binary Variables	Continuous Variables	Quadratic Terms
Original	240	30937	1440+2016c
0	240	31129	2016c
-1	288	31273	2016c
-3	384	31561	2016c
-5	480	31849	2016c
-8	624	32281	2016c

The original synergy problem for the 85-bus system with hierarchical data centers can not solved by the centralized method and also can not be directly solved by the distributed optimization method within the finite time. Through the reformulation by RNMDT, the near-optimal solutions can be derived by the proposed customized ℓ_1 -surrogate Lagrangian method. Simulation results in Table X indicate that the proposed distributed approach can derive acceptable results within an ideal agent-based average time of 3459.10s, which demonstrates the effectiveness and scalability of the proposed distributed approach in solving the large-scale, non-convex, and non-smooth synergy problems. These simulations are carried out on a personal computer to demonstrate feasibility. In real applications, more powerful computing facilities can further reduce the computation time.

TABLE X
DISTRIBUTED METHOD USING DIFFERENT PARAMETERS

	0	-1	-3	-5	-8
Value	-1321.60	-136.57	1297.26	1404.16	1465.45
Iteration	208	208	209	211	215
Time ₁ (s)	806.23	11860.28	14624.55	17413.45	20754.60
Time ₂ (s)	134.37	1976.71	2437.43	2902.24	3459.10

V. CONCLUSIONS

To address privacy leakage and combinatorial explosion concerns in the highly non-convex synergy problem of hierarchical data center penetrated power networks, we propose a near-optimal privacy-preserving distributed approach. The normalized multi-parametric disaggregation technique is leveraged to reformulate the non-convex mixed integer quadratically constrained quadratic programming into a mixed integer non-linear programming with the arbitrary accuracy. To further overcome the non-smoothness of the mixed integer problem, the customized ℓ_1 -surrogate Lagrangian relaxation method with convergence guarantees is proposed to solve the problem in a distributed privacy-preserving manner. Simulation results demonstrate that the proposed approach: i) derives high-quality near-optimal solutions and ensures convergence of the synergy problem; ii) preserves privacy of personal data for different agents in the integrated systems; iii) has high computational efficiency for the complicated synergy problem; iv) can leverage the flexible resource allocation capabilities of the hierarchical data center architecture, further facilitating peak load balancing in the power network. Future directions include developing measures of optimality gap and control mechanisms to boost performance of the customized ℓ_1 -surrogate Lagrangian method for synergy problems of the general and realistic integrated power networks.

REFERENCES

- [1] C. Fiandrino, D. Kliazovich, P. Bouvry, and A. Y. Zomaya, "Performance and energy efficiency metrics for communication systems of cloud computing data centers," *IEEE Transactions on Cloud Computing*, vol. 5, no. 4, pp. 738–750, 2015.
- [2] E. Ahvar, A.-C. Orgerie, and A. Lebre, "Estimating energy consumption of cloud, fog, and edge computing infrastructures," *IEEE Transactions on Sustainable Computing*, vol. 7, no. 2, pp. 277–288, 2019.
- [3] M. Xu, Z. Fu, X. Ma, L. Zhang, Y. Li, F. Qian, S. Wang, K. Li, J. Yang, and X. Liu, "From cloud to edge: a first look at public edge platforms," in *Proceedings of the 21st ACM Internet Measurement Conference*, 2021, pp. 37–53.
- [4] D. Kimovski, R. Mathá, J. Hammer, N. Mehran, H. Hellwagner, and R. Prodan, "Cloud, fog, or edge: Where to compute?" *IEEE Internet Computing*, vol. 25, no. 4, pp. 30–36, 2021.
- [5] D. Mytton and M. Ashtine, "Sources of data center energy estimates: A comprehensive review. joule 6, 2032–2056," 2022.
- [6] O. Han, T. Ding, M. Yang, W. Jia, X. He, and Z. Ma, "A novel 4-level joint optimal dispatch for demand response of data centers with district autonomy realization," *Applied Energy*, vol. 358, p. 122590, 2024.
- [7] Y. Zhang, A. Tsiligkaridis, I. C. Paschalidis, and A. K. Coskun, "Data center and load aggregator coordination towards electricity demand response," *Sustainable Computing: Informatics and Systems*, vol. 42, p. 100957, 2024.
- [8] Y. Cao, M. Cheng, S. Zhang, H. Mao, P. Wang, C. Li, Y. Feng, and Z. Ding, "Data-driven flexibility assessment for internet data center towards periodic batch workloads," *Applied Energy*, vol. 324, p. 119665, 2022.
- [9] Z. Liu, I. Liu, S. Low, and A. Wierman, "Pricing data center demand response," *ACM SIGMETRICS Performance Evaluation Review*, vol. 42, no. 1, pp. 111–123, 2014.
- [10] Y. Weng, Y. Liu, R. L. T. Lim, and H. D. Nguyen, "Distributed energy resource exploitation through co-optimization of power system and data centers with uncertainties during demand response," *Sustainability*, vol. 15, no. 14, p. 10995, 2023.
- [11] Z. Liu, A. Wierman, Y. Chen, B. Razon, and N. Chen, "Data center demand response: Avoiding the coincident peak via workload shifting and local generation," in *Proceedings of the ACM SIGMETRICS/international conference on Measurement and modeling of computer systems*, 2013, pp. 341–342.
- [12] Y. Xiao, A. C. Zhou, X. Yang, and B. He, "Privacy-preserving workflow scheduling in geo-distributed data centers," *Future Generation Computer Systems*, vol. 130, pp. 46–58, 2022.
- [13] W. Li, T. Qian, W. Zhao, W. Huang, Y. Zhang, X. Xie, and W. Tang, "Decentralized optimization for integrated electricity–heat systems with data center based energy hub considering communication packet loss," *Applied Energy*, vol. 350, p. 121586, 2023.
- [14] A. Rabiee and M. Parniani, "Voltage security constrained multi-period optimal reactive power flow using benders and optimality condition decompositions," *IEEE Transactions on Power Systems*, vol. 28, no. 2, pp. 696–708, 2012.
- [15] T. Erseghe, "Distributed optimal power flow using admm," *IEEE transactions on power systems*, vol. 29, no. 5, pp. 2370–2380, 2014.
- [16] D. Hur, J.-K. Park, and B. H. Kim, "Evaluation of convergence rate in the auxiliary problem principle for distributed optimal power flow," *IEEE Proceedings-Generation, Transmission and Distribution*, vol. 149, no. 5, pp. 525–532, 2002.
- [17] A. Engelmann, Y. Jiang, T. Mühlfordt, B. Houska, and T. Faulwasser, "Toward distributed opf using aladin," *IEEE Transactions on Power Systems*, vol. 34, no. 1, pp. 584–594, 2018.
- [18] L. Yu, T. Jiang, and Y. Zou, "Distributed real-time energy management in data center microgrids," *IEEE Transactions on Smart Grid*, vol. 9, no. 4, pp. 3748–3762, 2016.
- [19] G. Zhang, S. Zhang, W. Zhang, Z. Shen, and L. Wang, "Distributed energy management for multiple data centers with renewable resources and energy storages," *IEEE Transactions on Cloud Computing*, vol. 10, no. 4, pp. 2469–2480, 2020.
- [20] A. C. Zhou, R. Qiu, T. Lambert, T. Allard, S. Ibrahim, and A. E. Abbadi, "Pgprel: an end-to-end system for privacy-preserving graph processing in geo-distributed data centers," in *Proceedings of the 13th Symposium on Cloud Computing*, 2022, pp. 386–402.
- [21] W. Fan, J. He, M. Guo, P. Li, Z. Han, and R. Wang, "Privacy preserving classification on local differential privacy in data centers," *Journal of Parallel and Distributed Computing*, vol. 135, pp. 70–82, 2020.
- [22] A. Murray, T. Faulwasser, and V. Hagenmeyer, "Mixed-integer vs. real-valued formulations of battery scheduling problems," *IFAC-PapersOnLine*, vol. 51, no. 28, pp. 350–355, 2018.
- [23] A. Murray, A. Engelmann, V. Hagenmeyer, and T. Faulwasser, "Hierarchical distributed mixed-integer optimization for reactive power dispatch," *IFAC-PapersOnLine*, vol. 51, no. 28, pp. 368–373, 2018.
- [24] K. Sun, M. Sun, and W. Yin, "Decomposition methods for global solutions of mixed-integer linear programs," *arXiv preprint arXiv:2102.11980*, 2021.
- [25] Y. Chen, Q. Guo, and H. Sun, "Decentralized unit commitment in integrated heat and electricity systems using sdm-gs-alm," *IEEE Transactions on Power Systems*, vol. 34, no. 3, pp. 2322–2333, 2018.
- [26] N. Boland, J. Christiansen, B. Dandurand, A. Eberhard, and F. Oliveira, "A parallelizable augmented lagrangian method applied to large-scale non-convex-constrained optimization problems," *Mathematical Programming*, vol. 175, pp. 503–536, 2019.
- [27] S. Sharma and Q. Li, "A novel decentralized algorithm for coordinating the optimal power and traffic flows with evs based on variable inner loop selection," *arXiv preprint arXiv:2305.04124*, 2023.
- [28] S. Sharma, Q. Li, and W. Wei, "An enhanced sd-gs-al algorithm for coordinating the optimal power and traffic flows with evs," *IEEE Transactions on Smart Grid*, 2024.
- [29] M. A. Bragin, P. B. Luh, B. Yan, and X. Sun, "A scalable solution methodology for mixed-integer linear programming problems arising in automation," *IEEE Transactions on Automation Science and Engineering*, vol. 16, no. 2, pp. 531–541, 2018.
- [30] F. Si, Y. Han, J. Wang, and Q. Zhao, "Connectivity verification in distribution systems using smart meter voltage analytics: A cloud-edge collaboration approach," *IEEE Transactions on Industrial Informatics*, vol. 17, no. 6, pp. 3929–3939, 2020.
- [31] J. Li, C. Gu, Y. Xiang, and F. Li, "Edge-cloud computing systems for smart grid: state-of-the-art, architecture, and applications," *Journal of Modern Power Systems and Clean Energy*, vol. 10, no. 4, pp. 805–817, 2022.

- [32] G. Binetti, A. Davoudi, F. L. Lewis, D. Naso, and B. Turchiano, "Distributed consensus-based economic dispatch with transmission losses," *IEEE Transactions on Power Systems*, vol. 29, no. 4, pp. 1711–1720, 2014.
- [33] L. Gan, N. Li, U. Topcu, and S. H. Low, "Exact convex relaxation of optimal power flow in tree networks," *arXiv preprint arXiv:1208.4076*, 2012.
- [34] M. M.-U.-T. Chowdhury, M. S. Hasan, K. Murari, and S. Kamalasadan, "Socp based novel opf analysis model for ac-dc hybrid power distribution networks," in *2023 IEEE International Conference on Power Electronics, Smart Grid, and Renewable Energy (PESGRE)*. IEEE, 2023, pp. 1–6.
- [35] M. Abbasi, E. Mohammadi-Pasand, and M. R. Khosravi, "Intelligent workload allocation in iot–fog–cloud architecture towards mobile edge computing," *Computer Communications*, vol. 169, pp. 71–80, 2021.
- [36] M. Z. Chowdhury, M. Shahjalal, S. Ahmed, and Y. M. Jang, "6g wireless communication systems: Applications, requirements, technologies, challenges, and research directions," *IEEE Open Journal of the Communications Society*, vol. 1, pp. 957–975, 2020.
- [37] L. Chen, S. Zhou, and J. Xu, "Computation peer offloading for energy-constrained mobile edge computing in small-cell networks," *IEEE/ACM transactions on networking*, vol. 26, no. 4, pp. 1619–1632, 2018.
- [38] R. Lin, Z. Zhou, S. Luo, Y. Xiao, X. Wang, S. Wang, and M. Zukerman, "Distributed optimization for computation offloading in edge computing," *IEEE Transactions on Wireless Communications*, vol. 19, no. 12, pp. 8179–8194, 2020.
- [39] J. Zhang, D. Qin, Y. Ye, Y. He, X. Fu, J. Yang, G. Shi, and H. Zhang, "Multi-time scale economic scheduling method based on day-ahead robust optimization and intraday mpc rolling optimization for microgrid," *IEEE Access*, vol. 9, pp. 140 315–140 324, 2021.
- [40] Y. Liu, X. Wei, J. Xiao, Z. Liu, Y. Xu, and Y. Tian, "Energy consumption and emission mitigation prediction based on data center traffic and pue for global data centers," *Global Energy Interconnection*, vol. 3, no. 3, pp. 272–282, 2020.
- [41] A. Haywood, J. Sherbeck, P. Phelan, G. Varsamopoulos, and S. K. Gupta, "A sustainable data center with heat-activated cooling," in *2010 12th IEEE Intersociety Conference on Thermal and Thermomechanical Phenomena in Electronic Systems*. IEEE, 2010, pp. 1–7.
- [42] R. Alshahrani and H. Peyravi, "Modeling and simulation of data center networks," in *Proceedings of the 2nd ACM SIGSIM Conference on Principles of Advanced Discrete Simulation*, 2014, pp. 75–82.
- [43] Z. Wang, W. Wei, J. Z. F. Pang, F. Liu, B. Yang, X. Guan, and S. Mei, "Online optimization in power systems with high penetration of renewable generation: Advances and prospects," *IEEE/CAA Journal of Automatica Sinica*, vol. 10, no. 4, pp. 839–858, 2023.
- [44] Y. Li, S. Xia, M. Zheng, B. Cao, and Q. Liu, "Lyapunov optimization-based trade-off policy for mobile cloud offloading in heterogeneous wireless networks," *IEEE Transactions on Cloud Computing*, vol. 10, no. 1, pp. 491–505, 2019.
- [45] R. Urgaonkar and M. J. Neely, "Opportunistic scheduling with reliability guarantees in cognitive radio networks," *IEEE transactions on mobile computing*, vol. 8, no. 6, pp. 766–777, 2009.
- [46] T. Andrade, N. Belyak, A. Eberhard, S. Hamacher, and F. Oliveira, "The p-lagrangian relaxation for separable nonconvex miqcqp problems," *Journal of Global Optimization*, vol. 84, no. 1, pp. 43–76, 2022.
- [47] A. Mitsos, B. Chachuat, and P. I. Barton, "McCormick-based relaxations of algorithms," *SIAM Journal on Optimization*, vol. 20, no. 2, pp. 573–601, 2009.
- [48] R. T. Rockafellar and R. J.-B. Wets, *Variational analysis*. Springer Science & Business Media, 2009, vol. 317.
- [49] R. T. Rockafellar, "Level sets and continuity of conjugate convex functions," *Transactions of the American Mathematical Society*, vol. 123, no. 1, pp. 46–63, 1966.
- [50] M. A. Bragin, P. B. Luh, J. H. Yan, N. Yu, and G. A. Stern, "Convergence of the surrogate lagrangian relaxation method," *Journal of Optimization Theory and applications*, vol. 164, pp. 173–201, 2015.
- [51] A. Nedić and D. Bertsekas, "Convergence rate of incremental subgradient algorithms," *Stochastic optimization: algorithms and applications*, pp. 223–264, 2001.
- [52] R. D. Zimmerman, C. E. Murillo-Sánchez, and R. J. Thomas, "Matpower: Steady-state operations, planning, and analysis tools for power systems research and education," *IEEE Transactions on power systems*, vol. 26, no. 1, pp. 12–19, 2010.
- [53] P. Jenkins, M. Elmnifi, A. Younis, and A. Emhamed, "Hybrid power generation by using solar and wind energy: case study," *World Journal of Mechanics*, vol. 9, no. 04, pp. 81–93, 2019.
- [54] J. Gao, R. Chang, Z. Yang, Q. Huang, Y. Zhao, and Y. Wu, "A task offloading algorithm for cloud-edge collaborative system based on lyapunov optimization," *Cluster Computing*, vol. 26, no. 1, pp. 337–348, 2023.
- [55] N. Group, "Day-ahead locational marginal prices of uk electricity market," <https://www.nordpoolgroup.com/en/Market-data/1/GB/Auction-prices/UK/Hourly/?view=table>, accessed 2023.12.01.
- [56] Z. Tong, J. Cai, J. Mei, K. Li, and K. Li, "Dynamic energy-saving offloading strategy guided by lyapunov optimization for iot devices," *IEEE Internet of Things Journal*, vol. 9, no. 20, pp. 19 903–19 915, 2022.
- [57] J. Liu, "load and generation data for the data center," <https://github.com/johnny-ee/data-center.git>, 2024.
- [58] S. Boyd, N. Parikh, E. Chu, B. Peleato, J. Eckstein *et al.*, "Distributed optimization and statistical learning via the alternating direction method of multipliers," *Foundations and Trends® in Machine learning*, vol. 3, no. 1, pp. 1–122, 2011.